



Drivers of variations in the vertical profile of ozone over Summit Station, Greenland: An analysis of ozonesonde data

Shima Bahramvash Shams¹, Von P. Walden¹, Samuel Oltmans², Irina Petropavlovskikh², Bryan Johnson², Patrick Cullis², Chance W. Sterling², Laura Thölix³, Quentin Errera⁴, and Rigel Kivi⁵

5 ¹Laboratory of Atmospheric Research, Department of Civil and Environmental Engineering, Washington State University, Pullman, Washington, USA

²National Oceanic and Atmospheric Administration, Global Monitoring Division, Boulder, Colorado, USA

³Climate Research, Finnish Meteorological Institute (FMI), Helsinki, Finland

⁴Belgian Institute for Space Aeronomy, Uccle, Belgium

10 ⁵Space and Earth Observation Centre, Finnish Meteorological Institute, Sodankylä, Finland

Correspondence to: Shima Bahramvash Shams (s.bahramvashshams@wsu.edu)

Abstract. Understanding the drivers of atmospheric ozone variations in the Arctic is difficult because there are few long-term records of vertical ozone profiles in this region. We present 12 years of ozone profiles over Summit Station, Greenland (72.6 N, 38.4 W; 3200 meters) that were measured from 2005 to 2016. These profiles are subjected to data screening and are
15 extended to 60 km using a robust extrapolation method. The total column ozone and the partial column ozone in four atmospheric layers (troposphere to upper stratosphere) are analyzed. The monthly mean total column ozone reaches a maximum of about 400 DU in April, then decreases to minimum values between 275 and 300 DU in the late summer and early fall. The partial column ozone values peak at different times between late winter and early summer. There is a positive trend in the total column that is likely due to increases in springtime ozone, however, these trends are not robust given the
20 short period of record. A stepwise multiple regression analysis is performed to determine the primary drivers of ozone variations over Summit Station. This analysis shows that the variations in total column ozone are due primarily to changes in the tropopause pressure, the quasi-biennial oscillation (QBO), and the volume of polar stratospheric clouds. The eddy heat flux is also important for variations in the partial column ozone in the different altitude regions. The importance of the QBO appears to be a unique characteristic for ozone variations over the Greenland Ice Sheet (when compared to other nearby
25 Arctic Stations) and may be related to the fact that Greenland is particularly sensitive to the phase of the QBO.

1 Introduction

There is great interest in atmospheric ozone globally since the inception of the Montreal Protocol in 1987. Various parameters influence atmospheric ozone concentrations including dynamical variability (Fusco and Salby, 1999; Holton et al., 1995; Kivi et al., 2007; Rao et al., 2004; Rex, 2004), photolysis involving photochemical reactions (Bottenheim et al.,
30 1986; 2002; Sumner and Shepson, 1999; Van Dam et al., 2015; Yang et al., 2010), climate variables (Rex, 2004), and anthropogenic emissions of gases that interact with ozone (Cooper et al., 2010; Horowitz, 2006; Van der A et al., 2008).



Studies show that the mean total column ozone decreased from 1997 to 2003 globally (e.g., Newchurch, 2003), but some reports show that ozone depletion has recently decreased due to the ramifications of the Montreal Protocol (Weatherhead and Andersen, 2006; WMO, 2014; Steinbrecht et al., 2017; Weber et al., 2018). Recent work shows evidence of decreases in lower stratospheric ozone from 1998 to 2016 (Ball et al., 2018). Because of these changes, it is important to monitor ozone variability at many locations globally and to determine the causes of the variability.

During winters with persistent westerly zonal winds in the Tropics, planetary-scale Rossby waves propagate from the troposphere to the stratosphere. These winds are related to the tropical quasi-biennial oscillation (QBO) (Ebdon 1975; Holton and Tan, 1980). The interactions of these waves with the stratosphere modulate a meridional mass circulation towards the polar regions called the Brewer-Dobson circulation (Lindzen and Holton, 1968; Holton and Lindzen, 1972; Wallace, 1973; Holton et al., 1995). The location of the zero-wind line (latitude where the zonal wind speed is zero relative to the ground) is an important indicator of the strength of this circulation (Holton and Lindzen, 1972; Holton and Tan, 1980). During the easterly phase of the QBO, the zero-wind line shifts north, facilitating the propagation of planetary waves into the Arctic polar vortex. This creates a weakened vortex that increases the transport of relatively warm, ozone-rich air into the Arctic (Holton and Tan, 1982). The warmer temperatures also lead to less photochemical loss of ozone in the stratosphere (Rex, 2004; Shepherd, 2008). Conversely, during the westerly phase of the QBO, the propagation of planetary waves between the Tropics and the Arctic decreases, and the polar vortex is strengthened resulting in lower temperatures and increased probability of photochemical ozone loss. Thus, dynamical processes and the state of the polar vortex are important factors that determine ozone amounts in the Arctic.

Although there is strong observational evidence to support this teleconnection between the tropical and arctic atmospheres, a complete theoretical explanation has proved difficult (Anstey and Shepherd, 2014). The interaction of the background zonal mean wind and planetary waves is not completely understood, which makes it difficult to ascribe, in detail, how atmospheric dynamics affect the polar vortex. Furthermore, these effects depend on location and can also affect different portions of the atmosphere (Stahelin et al., 2001; Rao, 2003; Rao et al., 2004; Yang et al., 2006; Vigouroux et al., 2008; 2015). Thus, detailed analyses of the vertical structure of ozone are needed at various locations in the Arctic to fully understand the variability of ozone concentrations. This situation is exacerbated by both the lack of observations at high latitudes, as well as the difficulty of making quality measurements during winter; many remote sensing instruments for measuring ozone depend on solar radiation (Bowman, 1989; Hasebe, 1980; Vigouroux et al., 2008; 2015). Despite its importance, much uncertainty still exists in understanding the temporal and spatial variability of ozone (McIntyre, 1989; Stahelin, 2001; Jin et al., 2006; Manney et al., 2011).

One of the most important and reliable instruments for measuring the vertical profile of ozone is the ozonesonde. These instruments can be launched year-round and can provide valuable information for validation of remote sensing instruments aboard satellites. The Global Monitoring Division (GMD) of the National Oceanic and Atmospheric Administration (NOAA) launches ozonesondes routinely and have used the data to study trends, patterns, and the vertical distribution of ozone from many locations (Logan, 1994; Steinbrecht et al., 1998; Logan et al., 1999; Solomon et al., 2005; Miller et al.,



2006). Ozonesonde profiles from various Arctic stations have been used to study the climatology of the ozone cycle (Rao et al., 2004), the vertical distribution of ozone and its dependence on different proxies (Rao, 2003; Tarasick, 2005; Kivi et al., 2007; Gaudel et al., 2015), trends and annual cycles of ozone (Christiansen et al., 2017), the variability of ozone due to climate change (Rex, 2004), ozone loss and relation to dynamical parameters (Harris et al., 2010), the difference of ozone depletion in the Arctic and Antarctic (Solomon et al., 2014), and to evaluate other sensors measurements (McDonald et al., 1999; Vigouroux et al., 2008; Ancellet et al., 2016).

In spite of this, the long record of ozonesonde launches (2005-2017) by NOAA GMD has never been used to study the long-term variability of tropospheric and stratospheric ozone over Summit Station, Greenland (72.6 N, 38.4 W; 3200 meters). Summit Station is located in central Greenland atop the Greenland Ice Sheet (GrIS) and is the drilling site of the GISP2 ice core. Over the past few decades, near-surface temperatures over the GrIS have increased, which has resulted in increased snowmelt and runoff (Box and Cohen, 2006; Ettema et al., 2009; Hanna et al., 2013). It is also a location that is affected at times by pollution from mid-latitudes (Shindell et al., 2008). Greenland is in a unique location in the Arctic that is particularly sensitive to changes in the QBO [see Figure 2a of Antsey and Shepherd, (2014)]. In fact, the North Atlantic sector (0 to 60 W longitude) is the only Arctic location where the westerly-minus-easterly January mean 1000 hPa geopotential height field is statistically significant [see Figure 2a of Antsey and Shepherd, (2014)], indicating the sensitivity of this region to changes in the QBO.

In this study, we use 11 years of ozonesonde measurements (from 2005 to 2016) to document the vertical structure of ozone over Summit Station. In section 2, we describe the ozonesonde measurements and the data screening that was performed on these measurements. Section 3 describes how the ozonesonde measurements are combined with climatology of the upper atmosphere to create vertical profiles from 0 to 60 km. Section 4 discusses the results of the data analysis including determination of the seasonal and annual cycles of total ozone, as well as the cycles of partial ozone in four atmospheric layers that represent the troposphere, and lower, middle, and upper stratosphere. This section also determines the dependence of ozone over Summit Station on various ozone proxies using multiple regression (Appenzeller et al., 2000; Brunner et al., 2006; Kivi et al., 2007; Vigouroux et al., 2015; Steinbrecht et al., 2017). Section 5 presents the conclusions of this research.

25 **2 Data**

Summit Station, Greenland is chosen as the study area for this research because there is a long history of ozonesonde observations at this location. Figure 1 shows the location of Summit atop the Greenland Ice Sheet (GrIS). Table 1 lists the geographic coordinates and elevation of Summit, as well as Ny-Ålesund, Svalbard and Kiruna, Sweden, which are other sites that are discussed in this paper.

30 The initial focus of NOAA GMD's ozonesonde program at Summit was to measure ozone profiles to estimate the ozone concentration in the stratosphere. These measurements were started in February 2005 and continue until the summer of 2017. The data used in this study span 11 annual cycles from February 2005 through June 2016. We have chosen this time period



partly because this is the time period of the ozone proxies that are used for analysis. Ozonesondes were typically launched once per week except during the MATCH campaign when the frequency was temporarily increased to one every few days (Von Hobe et al. 2013). The ozonesonde profiles are available for download at NOAA's Earth System Research Laboratory. The ozonesondes use an electrochemical concentration cell (ECC) to measure ozone (Komhyr, 1986; Komhyr et al., 1989; Johnson et al., 2002; Deshler et al., 2008, Deshler et al., 2017, Sterling et al., 2017). The ozonesondes were manufactured by Environmental Science (EN-SCI) and used a sensing solution of neutral buffered 1% potassium iodide. The Strato telemetry software was used until the summer of 2014, then SkySonde was used thereafter. The raw data were also processed using SkySonde; details of ozonesonde homogenization can be found in Sterling et al. (2017). The ozonesonde were flown with a Vaisala RS80 radiosonde from 2005 to June 2014 and then an InterMet radiosonde until the end of the study period; both types of radiosondes measured temperature, pressure, and relative humidity. The profiles have been interpolated by NOAA GMD to a standard altitude grid with 100-meter spacing. The uncertainty in ozone concentration is $\pm (5 - 10)\%$ up to 30 km (Smit et al., 2007).

Data screening was performed on each ozonesonde used in this study. First, the maximum height reached by all of the ozonesondes is examined, because this is an important parameter that affects the calculation of the total column ozone. Figure 2a shows a histogram of the maximum height of the ozonesondes for the entire 11-year period. Most of the ozone profiles have maximum heights of 30 km or greater, but there is a significant fraction with maximum heights below 20 km. This bi-modal distribution is caused partly by the fact that the burst altitude of the balloons that carry the sondes depends on season; lower maximum altitudes are achieved in the extreme cold experienced during winter. To keep the uncertainty in the calculation of total column ozone acceptable, only ozonesondes that reached a maximum height of greater than 18 km were used in this study; profiles with maximum heights below 18 km were eliminated from further analysis. This reduces the uncertainty induced by using climatology to extrapolate the profile vertically through portions of the atmosphere that have appreciable ozone. Two ozonesonde profiles reached a maximum altitude of 50 km and were removed from further analysis due to erroneous readings from the pressure sensor.

Another data screening issue is related to missing data in the ozonesonde profiles. Most of the missing values occur at high altitudes because the ozonesonde ceased to report valid measurements after reaching some height. There were also some missing data in between valid ozone measurements. Figure 2b shows a histogram of the percentage of missing data in each profile; note that the vertical scale is logarithmic. Only a small fraction of the profiles has significant missing values. In this study, profiles that have a percentage of missing data greater than 40% are eliminated from further analysis. In the remaining profiles, if missing values occurred between valid ozone measurements, the profile was interpolated to fill the missing data. Table 2 lists the characteristics of the ozonesondes used in this study. After applying the data screening, Table 2 indicates that at least 25 ozonesondes are retained for analysis in each month, which satisfies the requirement for calculating a meaningful monthly-mean profile (Logan et al., 1999).

Figure 3 shows all of the screened profiles. Note that this plot is based on available screened ozonesondes and the time gaps between sondes are ignored. The seasonal dependence of the maximum height reached by the individual ozonesondes can



clearly be seen, with lower maximum heights in winter. The data are displayed as mixing ratios in ppmv and, therefore, are not indicative of the total amount of ozone as a function of altitude.

3 Methods

The total column abundance of ozone in the vertical profile is a useful parameter for understanding the amount of ozone in the atmosphere. The ozone column density is traditionally defined using the Dobson Unit (DU), which is the thickness of compressed gas in the atmospheric profile in units of 10 μm at standard temperature and pressure, 1 DU is equivalent to 1 milli-atm-cm, or 2.69×10^{16} molecules/cm². The total column ozone (TCO) in DU can be calculated as

$$TCO = \sum_{i=1}^n \frac{(VMR \cdot 10^{-6})_i P_i V_0}{R_d T_i MW_{air} \cdot 10^{-5}} \Delta h_i, \quad (1)$$

where i designates the i^{th} layer of the atmosphere, VMR_i , P_i , and T_i are the volume mixing ratio (ppmv), pressure (P_i), and temperature (K) of the layer obtained from the ozonesonde, R_d is the gas constant for dry air [287 Pa m³ K⁻¹ kg⁻¹], V_0 is the standard volume [22.4136 $\cdot 10^{-3}$ m³ mol⁻¹], and MW_{air} is the molecular weight of dry air [28.9644 $\cdot 10^{-3}$ kg mol⁻¹]. The factor 10^{-6} is a conversion factor between ppmv and mole/mole for ozone mixing ratio. Δh_i is the thickness of the atmospheric layer in 100 m increments. The factor 10^{-5} in the denominator is a conversion factor between meter and 10 micron. The ozone column for a single layer can be found using Eq. 1 by summing over an individual layer.

To provide realistic values of total column ozone, the screened ozonesondes must be integrated over all layers of the atmosphere that contain appreciable ozone. Therefore, the ozonesondes were extrapolated to 60 km using climatological profiles that are appropriate for the atmosphere over Greenland. To assess the uncertainty in applying the climatological data, four different extrapolation methods were used. Two climatological ozone profiles were used, along with two different methods of merging these profiles to the actual measured ozonesonde profile.

We use both the monthly climatological profiles from McPeters and Labow (2012) (referred to here as the ML climatology) and one constructed from monthly averages using the 11 years of actual ozonesonde profiles. In the first case, the monthly ozone profile from the ML climatology is extended above each individual sonde profile up to 60 km. [The ML climatology for each month was estimated on a 10-degree latitude grid using data from the Microwave Limb Sounder on Aura (2004–2010) and ozonesonde data (1988–2010) (McPeters and Labow, 2012)]. In the second case, the 11-year monthly averages are used above each individual sonde profile, and then the associated ML climatology for the given month is used to 60 km. The amount of data used from the 11-year averages depends on the maximum altitude reached by the individual ozonesondes and the maximum altitude of the 11-year average itself, both of which depend on season. For example, a sounding that only reached 20 km would be extrapolated over a large altitude range of 10 to 15 km, using the 11-year monthly average. However, another sounding that reached a relatively high altitude, say 30 km, might not be extrapolated at all by the 11-year monthly average. But the purpose here is to use as much of the actual data from the ozonesondes as possible and to compare those profiles to those constructed by simply using the ML climatology.



An additional consideration is how to merge the different ozone profiles together. This was done in two ways. First, the profiles were constructed by simply attaching the different vertical sections together with no attempt to smooth the transitions between the different sections. In certain cases, this caused large discontinuities in the profiles at the boundaries between the vertical sections. To mitigate this, a second method was used that merged the upper level profiles by scaling
5 them to the lower section, which ensured smooth transitions between each section. The scaling was accomplished by first determining the ratio of the upper-most ozone value from the ozonesonde and the lower-most value of the climatological profile. The climatological profile is then scaled by this ratio (the scale factor) to merge it with the ozonesonde profile.

To assess the differences in the four methods of constructing the upper ozone profile, Figure 4 shows the monthly average total column ozone for the 11-year period calculated from the four different constructed profiles. The values shown along the
10 top axis of the graph are the monthly averages of the standard deviations of the TCO of the four constructed profiles. Figure 4 shows that these methods agree well for most of the year, indicating that each of the methods provides reasonable values of total column ozone. As expected, the standard deviation of different methods is large in January and December when the ozonesondes have the lowest average maximum height (see Table 2). For these months, a greater portion of the individual ozone profiles had to be constructed from climatology and, therefore, the different construction methods are more uncertain.
15 The lack of an absolute reference for stratospheric ozone over Greenland make it difficult to choose which method is best. Therefore, the average of the four methods is used for subsequent analysis in this study.

Figure 4 also shows the multi-year averages of total column ozone measured at the nearby Arctic stations of Kiruna and Ny-Ålesund, which were retrieved from measured by solar Fourier Transform Spectroscopy [from Vigouroux et al., 2008], which are discussed below in Section 4. TCO at Kiruna is similar to Summit Station except in winter and early spring. In
20 most months, the TCO at Summit is less than that measured at Ny-Ålesund. The different geographical locations and the higher elevation of Summit Station likely contribute to these disparities. (For comparison, the ML climatological ozone profile has about 1.5% of total column ozone (about 6 DU) in the lowest 3 km of atmosphere.) However, the different time periods and locations of the Kiruna and Ny-Ålesund datasets might also contribute to this disparity. Detailed analysis of the vertical variation in TCO at these stations will be discussed further in the section 4.

To determine the drivers upon which the monthly average total column ozone at Summit depend, we use a stepwise multiple regression (SMR) model similar to that used by Appenzeller et al., 2000; Brunner et al., 2006; Kivi et al., 2007; Vigouroux et al., 2015; Steinbrecht et al., 2017. The model is briefly explained here, while the analysis and results are discussed below in Section 4. The model involves the use of various proxies that have been previously identified as important indicators of ozone concentrations in the troposphere and stratosphere. To facilitate comparisons to other locations, similar proxies are
30 used in this study that were used by (Brunner et al., 2006; Kivi et al., 2007; Vigouroux et al., 2015). Figure 5 shows time series of the proxies: tropopause pressure (TP), the Quasi-Biennial Oscillation at both 10 hPa and 30 hPa (QBO10; QBO30), volume of polar stratospheric clouds (VPSC), eddy heat flux (EHF), Arctic Oscillation (AO), equivalent latitude (EQL) at three potential temperature levels 370 K, 550 K, 960 K, solar flux (SF), and the El Niño-Southern Oscillation index (ENSO). (The monthly averaged values for TP, VPSC, and EHF are calculated using data from the dates of ozonesondes.) Table 3



lists the sources of these proxies. This list is similar to that used by previous studies (Brunner et al., 2006; Vigouroux et al., 2015) and contains variables that are known to influence ozone concentrations in the troposphere and stratosphere (Brunner et al., 2006; Vigouroux et al., 2015). Following Vigouroux et al (2015), the multiple regression model is given by:

$$Y(t) = A_0 + A_1 \cos\left(\frac{2\pi t}{12}\right) + A_2 \sin\left(\frac{2\pi t}{12}\right) + A_3 \cos\left(\frac{4\pi t}{12}\right) + A_4 \sin\left(\frac{4\pi t}{12}\right) + \sum_{k=5}^n A_k X(t)_k + \varepsilon(t), \quad (2)$$

- 5 where $Y(t)$ is the final regression model, t is the month (1 to 12), A_0 - A_4 are coefficients related to the seasonal cycle, A_k (when $k \geq 5$) are the coefficients related to the proxy time series $X(t)_k$, and ε is the residual (that is not explained by the combination of the seasonal cycle and the proxies). Any linear trend in the data is considered as one of the proxies using $X_k(t) = t$. The model is implemented using the following procedure. First, the seasonal cycle for the 11-year period is determined by finding the coefficients A_0 - A_4 . These terms are then subtracted from the original TCO time series to yield a
- 10 residual time series. Using the technique described in Section 7.4.2 of Wilks, 2011, stepwise regression (with forward selection) is then performed on the residual time series using the different proxies. To accomplish this, each proxy is regressed with the residual TCO time series, and the proxy that has the highest explained variance (R^2) is selected. This proxy [e.g., $A_5 X_5(t)$] is then included in a new fit to the residual TCO time series using multiple linear regression to create a new residual time series. This process is repeated until none of the remaining proxies increase the R^2 by more than 1%. To
- 15 be consistent with previous studies and to account for auto-correlation in the residuals, we applied the Cochrane-Orcutt transformation (Cochrane & Orcutt 1949; Vigouroux et al. 2015) to the final model, but it had an insignificant effect on the overall results. Therefore, it was not used to adjust the final regression model. The different proxies and their usefulness in explaining the variance of the time series of TCO are described below in section 4.4.

4 Results and Discussion

- 20 In this section, the 11-year record of ozonesonde profiles over Summit Station, Greenland is discussed. First, the vertical profiles of ozone and their temporal variation are described. This is followed by a brief comparison of the seasonal cycle of ozone over Summit to other nearby Arctic locations. The trends of ozone in various vertical sections of the atmosphere are discussed, while acknowledging that it is difficult to ascribe trends over such a short time period. Finally, we describe the results of the SMR analysis, which yields insight into the primary drivers of ozone variability over Greenland.

25 4.1 Vertical profiles

- Figure 6 shows profiles of the monthly average partial column ozone (PCO) in 100-meter layers over Summit Station, Greenland. The maximum PCO (in DU) occurs at about 20 km in all months. However, there is a significant dependence on the timing of the peak ozone amount (in DU) with the maximum peak value occurring in January and the lowest peak values in July, August, September, and October. There is also significant seasonal variation in the ozone between about 10 and 30
- 30 km, which greatly affects the total column ozone. As an example, even though the minimum average TOC occurs in October



(black dashed line in Figure 4), the peak of October's PCO is greater than that of June, July and September. This is because October has higher ozone around 20 km but lower ozone in both the upper and lower layers compared to June, July and September.

The differences between the monthly average profiles over Summit and the ML climatology are also plotted in Figure 6. The Summit ozone profiles have lower ozone than the climatology below 10 km. Between 10 km to 20 km, warmer/colder months show lower/higher ozone in sondes comparing to climatology. Between 20 km to 35 km, the ML climatology has lower values than the Summit ozonesondes. Above about 35 km, ozone profiles are merged with the ML climatology, therefore, the differences are close to zero. These differences justify the use of the average of the different methods to estimate the missing ozone at high elevations for each sonde, as described in Section 3.

10 4.2 Seasonal cycle

Figure 7a shows the seasonal variation of the PCO profiles in each 100-meter layer. The seasonal cycle in the profiles is apparent with maximum values occurring in spring between roughly 15 and 22 km. Minimum values occur in the summer and autumn with large decreases in ozone in the lower stratosphere between 10 and 25 km. These variations are similar to those reported previously for Arctic sites (e.g., Rao, 2003; Rao et al., 2004; Vigouroux et al., 2008; 2015). The values of springtime ozone are quite low over Summit in 2005 and especially in 2011. These were well documented as times of extreme ozone loss throughout the Arctic (Jin et al., 2006; Manney et al., 2011). The ozonesonde data from Summit confirm that these events also occurred over Greenland. Figure 7b shows the corresponding values of total column ozone for all of the screened ozonesondes in Dobson units and clearly shows the seasonal cycle, including the timing of the peaks and troughs in TCO throughout the year. For comparison, the daily values of TCO for the entire Arctic region (latitude > 63° N) are shown; these data were obtained from the NASA Ozone Watch produced by Paul A. Newman of Goddard Space Flight Center (<https://ozonewatch.gsfc.nasa.gov/NH.html>). The variation of TCO over Summit Station over this time period agrees well with the NASA Ozone Watch data, however, there are times when the TCO over Summit differs greatly (by as much as 50-100 DU) from the Arctic average.

Figure 8 shows the multi-year averages for four atmospheric layers: surface to 10 km, 10 to 18 km, 18 to 27 km, and 27 to 42 km. These layers were chosen to match those used by Vigouroux et al (2008). For the purpose of this study, the layers represent the troposphere, lower stratosphere, middle stratosphere, and upper stratosphere, respectively. (Note that the tropopause is low in the Arctic, so the layer from the ground to 10 km represents primarily values in the troposphere, but also contains some ozone from the lowest portion of the stratosphere. However, we refer to this layer here as the "troposphere" for convenience.) The values shown in Figure 8 are the partial column ozone (PCO) amounts, which are the column ozone in Dobson units that are contained within the respective atmospheric layers. The largest values of PCO occur in the layers of the lower (75-150 DU) and middle stratosphere (120-175 DU), which straddle the peak in column ozone amount around 20 km. The PCO in the troposphere and upper stratosphere range from 20-40 DU and 60-80 DU, respectively.



The seasonal cycle is different in the various atmospheric layers. The timing of the peak ozone at different altitudes is due to different physical processes that affect ozone concentrations. At Summit Station, the PCO values in the upper stratosphere peak later in the year with values of about 75-80 DU in May, June, and July. The values are about 10 to 20 DU higher than the minimum in October due to increased daylight in spring when photolysis equilibrium is reached (Crutzen, 1971). The PCO in the middle stratosphere peaks earlier in winter in January and February. This is due to accumulation of transported ozone from lower latitudes during wintertime caused by the Brewer-Dobson circulation (Staehelin et al., 2001). The PCO in the lower stratosphere peaks in March and represents the well-known springtime maximum in the Arctic, which is caused by winter accumulation that occurs before ozone transport to the troposphere (Rao, 2003; Rao et al., 2004; Staehelin et al., 2001). The PCO peaks in the troposphere in April, caused primarily by relatively large ozone concentrations between 6 and 10 km. However, this ozone appears to be transported downward in the troposphere later in the spring because concentrations peak between 4 and 6 km in May. The peak in the upper troposphere in April is likely caused by intrusion of ozone-rich air from the stratosphere. The subsequent intrusion of ozone into the troposphere later in the spring are likely the result of tropospheric folds that occur in mid to late spring (Holton et al., 1995; Van Haver et al., 1996). The greatest seasonal variation (shown as uncertainty bars in Fig. 7) is seen in the lower and middle stratosphere with values peaking in late winter and early spring, and then decreasing to minimum values in late summer and early autumn. The ozone variations seen in winter (Nov-Jan) in the upper stratosphere (27-42 km) may be due to poor statistical sampling because fewer sondes reach those altitudes in winter.

Figure 8 also shows the values of PCO based on FTS for Kiruna and Ny-Ålesund (from Vigouroux et al, 2008) and exhibit similar seasonal cycles to those at Summit. Vigouroux et al., 2008, only report values for March-September at Ny-Ålesund and January-November at Kiruna because measurements were only obtained during periods of sunlight. However, the amount of ozone in the troposphere is much less over Summit Station because of the high surface elevation of that site [roughly 3200 meters above sea level (asl)]. Kiruna is located at 580 meters asl; Ny-Ålesund is near sea level at 40 m asl. This effect is largest in the lowest layer, ground to 10 km, where the PCO at Kiruna and Ny-Ålesund are consistently 10-20 DU larger than at Summit.

4.3 Trends

Trends in the total column ozone over Summit Station, Greenland are now considered. It should be emphasized that determining significant trends using linear regression over such a short time period is of questionable value. For instance, the trends can be greatly influenced by the endpoints of the time series over which the regression is performed. Therefore, the following results should be interpreted with caution. Here we report the slope of the linear fit (trend) as well as the uncertainty in the slope. There is some confidence for trends that have a slope that is greater than the uncertainty in the slope. Figure 9 shows the TCO values for the multi-year (annual) and seasonal averages. (To be consistent with the SMR analysis, these averages were calculated using the time range of the proxies.) The trends in winter, spring, and summer are positive, but none of the trends is significant. There is a decreasing trend in fall in TCO (-1.18 DU/year), but with a comparable



uncertainty (± 1.24 DU/year). The regression slope for the annual values (1.26 DU/year) is positive and is greater than the uncertainty (± 0.87 DU/year), indicating a slight increase in the annual TCO over Summit Station from 2005 to 2016. However, caution should be used when interpreting the increase in TCO because of the short period of record (12 years).

4.4 Drivers of ozone variation over Greenland

5 To identify the drivers of ozone variations over Summit Station, Greenland, the SMR technique described in Section 3 is used. We refer back to Figure 5 and Table 3, which describe the proxies used to determine the causes of ozone variations. The most dominant source of ozone variation is the seasonal cycle, so the first step in the analysis is to remove this cycle. Figure 10 shows the values of total column ozone (top panel) and the partial ozone column values for each of the four altitude regions introduced in section 4.2 (bottom four panels). The seasonal cycle is determined by fitting the time series
10 with the first five terms in Eq. 2. These cycles are also shown in Figure 10. The first row of Table 4 (and the titles in Figure 10) shows that the seasonal cycle explains over 50% of the variance in both the total and partial column ozone values. The coefficient of determination, R^2 , for total column ozone is 0.68, or 68%.

The SMR analysis is then performed on the residual time series, which are determined by subtracting the seasonal cycles from the total and partial column ozone time series. Before the results of the SMR analysis are discussed, it is important to
15 note that the removal of the seasonal cycle likely decreases the influence of proxies that have seasonal variations. Figure 5 shows that this is mostly true for the eddy heat flux and, to a lesser degree, the volume of polar stratospheric clouds.

The SMR analysis is initiated by calculating the coefficient of determination (R^2) for each proxy using the residual time series. The best proxy at each step in the analysis is the one with the largest R^2 value, which is at least 1% higher than R^2 of previous step. Table 5 summarizes the results of the analysis for each time series. The list of proxies is in order of
20 importance (in descending order of R^2 values) and is different for each of the five residual time series. We also list the sign of the slope of the regression fit of each proxy in Table 5 to the left of the R^2 value (except for the QBO because this proxy involves multiple terms); the sign of the slope indicates positive or negative correlation between the proxy and the residual time series. The bottom row of Table 5 lists the cumulative R^2 value of all accepted proxies and, therefore, shows the variance explained by the selection of proxies. Figure 11 is a graphical representation of the results in Table 5. The time
25 trends were included in the regression analysis by using $A_k = 1$ in Eq. 2. A small positive trend was detected in total column because of low and mid stratospheric (10-27 km) layers, however, this should be interpreted with caution due to the short period of study.

Table 5 and Figure 11 show that tropopause pressure (TP) is the most important proxy for all of the time series except in the upper stratosphere (27-42 km). The seasonal cycle in TP is difficult to detect in Figure 5a, but the largest values of TP
30 generally occur in winter and spring; note that the y-axis in Figure 5a decreases upward, so large pressure values indicate lower height levels in the atmosphere. TP has been shown to correlate well with total column ozone (Appenzeller et al., 2000; Steinbrecht et al., 1998). Lower TP (higher tropopause height) leads to lower values of ozone (Steinbrecht et al., 1998). Tropopause height can also be increased due to lower stratosphere temperatures (Forster and Shine, 1997), which can



result in ozone depletion (Rex, 2004). An increase in tropopause height is also correlated with increases in tropospheric temperature, which can affect the ozone concentration via vertical transport. The transport of ozone to higher levels in the atmosphere can increase ozone destruction because photochemical reactions increase (when sunlight is available) (Steinbrecht et al., 1998).

5 Table 5 and Figure 11 show that the QBO is the second most important proxy in the lower (10-18 km) and middle stratosphere (18-27 km), and essentially tied for second (along with VPSC) for total column ozone. The QBO has been shown to be important for transport of ozone from the tropics to higher latitudes (Hasebe, 1980; Bowman, 1989; Thompson et al., 2002; Brunner et al., 2006; ; Nair et al., 2013; Anstey and Shepherd, 2014; Li and Tung, 2014; Steinbrecht et al., 2017;). Here two proxies of the QBO are used (Figures 5b, 5c): the zonal wind (in m s^{-1}) at 10 hPa (QBO10) and 30 hPa
10 (QBO30) at Singapore as in previous studies (Brunner et al., 2006; Anstey and Shepherd, 2014; Vigouroux et al., 2015). Choosing to characterize the QBO using winds at two pressure levels is supported by the review of Anstey and Shepard (2014), which states that there is currently no consensus as to what pressure level in the tropics has the greatest influence at high latitudes. To accommodate the approximate 28-month cycle of the QBO and the lag time of its effect, five coefficients (including sinusoidal terms) are used to model the combined effect of the QBO10 and QBO30 (Vigouroux et al., 2015). As
15 mentioned in the Introduction, the QBO modulates planetary-scale Rossby waves and consequently the poleward transport of ozone from the Tropics by shifting the zero wind line.

A close evaluation of the residual ozone and the QBO time series shows that the largest ozone values occur when the QBO is in the easterly phase. Under these conditions, the stratospheric circulation leads to increases in ozone over Greenland by both weakening the polar vortex and warming it up (Holton and Tan, 1980). In general, higher stratospheric temperatures in the
20 Arctic lead to less photochemical loss of ozone (Rex, 2004; Shepherd, 2008). On the other hand, the westerly phase of the QBO strengthens the polar vortex, which decreases stratospheric temperatures over Greenland and leads to ozone loss.

To our knowledge, no previous studies have focused on the effect of stratospheric dynamics on ozone over Greenland specifically. In spite of this, Greenland appears to be located in an area of the Arctic that is particularly sensitive to the QBO, which might explain why the QBO proxy explains a significant portion of the variance in the ozone residual time series over
25 Summit Station. Figure 2a of Anstey and Shepherd (2014) indicates that the stratosphere over Greenland exhibits the most extreme variability in westerly versus easterly phases of the QBO. Our results show that ozone over Summit Station is more dependent on the QBO phase than other nearby Arctic stations; see the analysis by Vigouroux et al (2015) for Ny-Ålesund and Kiruna. According to Anstey and Shepard's results (Figure 2a), the locations of both Ny-Ålesund and Kiruna should be influenced by the QBO phase, but to a lesser degree than Summit Station. It is important to note that the time series of ozone
30 variations over Ny-Ålesund and Kiruna were available only during sunlit times and, therefore, have data gaps during an important time when ozone fluctuations depend on the winter stratospheric circulation. Furthermore, the effect of the QBO on Arctic ozone is complicated, and its effect at different locations is an area of active research (Anstey and Shepherd,



2014). But long time series of the vertical profile of Arctic ozone are needed to more fully understand the connection to the QBO.

To investigate the robustness of the QBO proxy and its effect on the regression analysis, we removed the QBO from the list of proxies and re-calculated the SMR analysis to study the changes in final model. Inclusion of the QBO proxy increased the final model correlation coefficient of residuals by <1%, 12%, 32%, 21%, 12% in the 0-10 km, 10-18 km, 18-27 km, 27-42 km layers, and the Total Column respectively. The effect is greatest in the 18-27 and 27-42 km layers and decreases in importance lower in the atmosphere. This analysis shows that the QBO plays a significant role in explaining ozone variations over Greenland. Furthermore, no other proxy accounts for the ozone variance provided by the QBO proxy and, thus, the QBO is an important and unique contributor.

10 Polar stratospheric clouds in the Arctic atmosphere contribute to ozone loss through photochemistry (Rex et al, 2004; Brunner et al., 2006). In this study, the volume of polar stratospheric clouds is multiplied by effective equivalent stratospheric chlorine (EESC) to account for the modulation of VPSC by EESC (Brunner et al., 2006). The cumulative effect of VPSC has been shown to have a semi-linear relationship to ozone loss (Rex et al., 2004). To account for the cumulative effect on ozone, we use equation 4 from Brunner et al. (2006). For simplicity, we use the term VPSC here to refer to the collective effect that includes EESC and accumulation. This proxy is shown in Figure 5d. VPSC is the second most important proxy for TCO because of its influence on stratospheric layers (10-42 km) layers (Table 5). Lower stratospheric temperatures result in more polar stratospheric clouds, thus, large VPSC is an indicator of low stratospheric temperatures and a stronger polar vortex (Rex, 2004). The reduction in potential temperature is associated to ozone loss (Rex, 2004) and higher values VPSC are then negatively correlated with the total column ozone, which is confirmed by the negative slope of this proxy (Table 5).

The Brewer-Dobson circulation is one of the most important processes that impacts ozone transport from the Tropics to the Arctic (Staehelin et al., 2001). The seasonal cycle of ozone in the extratropics is caused, in part, by this circulation (Fusco and Salby, 1999). The vertical component of the Eliassen-palm flux and the eddy heat flux (EHF) are proportional to each other and are both good indicators of the Brewer-Dobson circulation (Brunner et al., 2006; Eichelberger, 2005; Fusco and Salby, 1999). In this study, the spatially-averaged EHF at 100 hPa over 45-75° N is used. The variation of EHF is shown in Figure 5e. As mentioned above, the seasonal variation of EHF is similar to that of ozone over Summit Station with maximum values in winter. Large values of EHF indicate higher wave forcing of stratospheric circulation, which weakens the polar vortex and leads to higher ozone (Fusco and Salby, 1999), therefore, Table 5 shows that the correlation between EHF and ozone is positive and it is the first most important proxy in upper stratosphere (27-42 km).

30 The other proxies, the Arctic Oscillation (AO) (Figure 5f), solar flux (Figure 5j), and the El-Niño Southern Oscillation (ENSO) (Figure 5k), have little influence on either the partial or total column ozone over Summit Station. The AO proxy also plays a minor role in the ozone variations over Summit Station, but has been tied to changes in the polar vortex and stratospheric circulation (Appenzeller et al., 2000). The AO is the third most important proxy in the lower stratosphere, but it does not significantly affect the TCO.



Equivalent latitude (EQL) can also affect the ozone concentration. Equivalent latitude is an index estimated based on potential vorticity (PV) that is indicative of isentropic ozone (air parcel) transportation between the lower stratosphere and upper troposphere (Danielsen, 1968; Butchart & Remsberg, 1986; Allen & Nakamura, 2003). Adiabatic vertical movement of air parcels changes the volume of an air parcel, which consequently changes the ozone mixing ratio. Moreover, isentropic horizontal advection can affect the ozone concentration when an air parcel is transported to a location with surrounding air that has different properties (Danielsen, 1968; Butchart and Remsberg, 1986; Salby and Callaghan, 1993; Allen and Nakamura, 2003, Wohltmann et al., 2005). We used equivalent latitude at three potential temperature levels of 370 K, 550 K, and 960 K. Monthly fluctuations of these levels are shown in Figures 5g, h, and i. The EQL proxies has been found insignificant contributor to ozone fluctuations at Summit Station. However, EQL at 960 K influenced the ozone within the tropospheric layer in spite of very little influence in the stratospheric layers and the total column ozone. Because of this, we believe that this effect is spurious and is not supported by any physical process, therefore, we removed this proxy from further analysis.

The solar flux and ENSO show insignificant contributions at any level in the atmosphere and the TCO. The solar flux and its 11-year cycle are known to influence stratospheric ozone concentrations (Newchurch, 2003; Brunner et al., 2006), but Figure 5g shows that the solar flux completes only one solar cycle during the relatively short time period of this study. However, the solar flux has been found to be a significant proxy in other regions of the Arctic with longer datasets (Vigouroux et al., 2015). The El Niño-Southern Oscillation (ENSO) is also an important proxy of ozone variations in many locations (Doherty et al., 2006; Randel et al., 2009). The time series of the multivariate ENSO index (MEI) is shown in Figure 5h. To investigate the effect of ENSO variations on ozone over Summit Station, the MEI was used with time lags between 0 and 4 months in a manner similar to Randel et al., 2009 and Vigouroux et al. 2015. None of the time-lagged MEI proxies affected the ozone variation over Summit Station. The physical mechanism between warm ENSO conditions and polar stratosphere warming is not fully understood yet, however, observations show that unusual convergence of EP flux follows a warm ENSO, which promote warming in the polar regions (Taguchi and Hartmann, 2006; Garfinkel and Hartmann, 2008). However, it is shown that the easterly phase of the QBO reduces the effect of a warm ENSO on the polar stratosphere (Garfinkel and Hartmann, 2007). This might be the reason that Greenland is not affected significantly by the ENSO effect via its modulation of the Arctic polar vortex; see Figures 6 and 8 in (Garfinkel and Hartmann, 2008).

Figure 12 shows the results of the final regression model. The final regression is calculated using the coefficients that were found by fitting the seasonal cycle and those determined in the SMR and then re-calculating Eq. 2. The final values of R^2 are shown as the bottom row in Table 4. By comparing the two rows in Table 4, the effect can be seen of how the SMR analysis explains additional variance beyond that of the seasonal cycle. The SMR analysis increases the R^2 values between 4 and 22% in the different altitude regions and 16% in the TCO.

Figure 12 shows that the final regression model fits the ozone variations well both in TCO and the PCO in the four altitude regions. Furthermore, it can be seen that the final regression model provides significantly more information than the seasonal cycle alone. Using Figure 11 and Table 5, we conclude that the tropopause pressure, QBO, and VPSC explain the majority of



ozone variations in the total column ozone. The tropopause pressure and QBO play major roles in the variation of ozone in the four different altitude regions, while VPSC, the eddy heat flux, and AO play minor roles.

It should be noted that the proxies may be correlated with each other (Appenzeller et al., 2000; Vigouroux et al., 2015). We calculated the covariance matrix for all combinations of the proxies used in the SMR model and found that most covariances are less than 0.20. However, certain combinations of the EHF, VPSC, and the EQL proxies are significantly correlated with each other; EHF-VPSC = 0.66, EQ370-EQ550 = 0.58, VPSC-EQ370 = 0.40, and EHF-EQ370=0.38. The EQL proxy did not contribute significantly to the final model, even if both EHF and VPSC were excluded from the analysis, thus, this correlation does not affect the overall analysis. The contribution of VPSC to the ozone fluctuations is greater than that of EHF, but removing VPSC did not improve the contribution of EHF. However, the inclusion of EHF slightly decreased the contribution of VPSC in troposphere. In spite of this, the SMR analysis is useful for understanding how the individual proxies explain the variance of ozone and for determining the primary drivers of variability in the residual time series of ozone. We also acknowledge that the regression model developed here is likely to be unsuitable for other Arctic locations due to the unique characteristics of Summit Station including its high altitude on the GrIS. Furthermore, other studies have shown that the analysis of ozone drivers depends significantly on the study location (Staehelin et al., 2001; Rao, 2003; Rao et al., 2004; Yang et al., 2006; Vigouroux et al., 2008; 2015).

5 Conclusions

To fully understand the ramifications of the Montreal Protocol, there is continued interest in global ozone concentrations. There is also continuing debate as to what controls Arctic ozone and what are the relative contributions of dynamics and photochemistry (Antsey and Shepard, 2014). Understanding what cause variations in Arctic ozone is particularly difficult because there are few long-term records of the vertical profile of ozone in this region. We present 12 years of vertical profiles of ozone over Summit Station, Greenland that were measured from 2005 to 2016 using ozonesondes launched by NOAA. These profiles are subjected to data screening and are extended to 60 km using four different extrapolation methods. The differences in the extrapolation are not significant, so the average of the four methods is used to create profiles that are used for further analysis.

The ozone profiles over Summit Station are used to examine ozone variations over the Greenland Ice Sheet. The total column ozone and the partial column ozone in four atmospheric layers are analyzed: surface to 10 km, 10-18 km, 18-27 km, and 27-42 km. The monthly mean total column ozone reaches a maximum of about 400 DU in April, then decreases to minimum values between 275 and 300 DU in the late summer and early fall. In the tropopause (surface to 10 km), the partial column ozone increases during spring to a maximum in April because of stratosphere-troposphere exchange caused by tropopause folding. In the lower to middle stratosphere, the ozone increases from fall into the winter with peak values occurring in late winter or early spring. The ozone then decreases during the spring and summer. This cycle is consistent with winter accumulation of ozone followed by the springtime breakup of the polar vortex and a return to photolysis



equilibrium in summer. In the upper stratosphere, the partial column ozone peaks in late spring or early summer, which is consistent with ozone production associated with solar illumination and photolysis.

The multi-year trend in total column ozone is positive over the 12-year period of this study. This is likely caused by a similar trend in the springtime ozone, which is also positive. Because the ozone amounts are higher in spring, the positive trend in spring dominates a negative trend in fall when the ozone concentrations are at a minimum. However, we acknowledge the large uncertainty associated with these trends due to the short period of study (12 years).

Stepwise multiple regression analysis is performed to determine the dominant proxies that affect ozone variations over Summit Station. After removing the seasonal cycle, the SMR analysis was successful in identifying proxies that explained a significant portion of the ozone variance. The coefficient of determination (R^2) of the final regression model was 0.84 for total column ozone and between 0.69 and 0.84 for the different altitude regions, which was a significant improvement over fitting simply with a seasonal cycle. The tropopause pressure, quasi-biennial oscillation, and the volume of polar stratospheric clouds are important proxies for the total column ozone. The partial column ozone amounts in the different altitude regions depend primarily on tropopause pressure and quasi-biennial oscillation but also somewhat on the volume of polar stratospheric clouds, eddy heat flux, arctic oscillation. Interestingly, equivalent latitude, the solar flux, and El Niño-Southern Oscillation proxies are not important for ozone variations over Summit Station. We suspect that a longer period of study is required to fully analyze the effect of solar flux on ozone fluctuations. The relative importance of the QBO at all altitudes may be related to the fact that Greenland lies in a region that is particularly sensitive dynamically to variations in the phase of the QBO winds (Anstey and Shepherd, 2014). Thus, the primary drivers of ozone variations over the Greenland Ice Sheet may be unique when compared to other nearby Arctic stations, like Ny-Ålesund and Kiruna. However further study is required because Ny-Ålesund and Kiruna lack measurements during the polar night and, thus, a full seasonal cycle. This is especially important because winter is a critical period for ozone accumulation and transportation to the Arctic. Thus, additional studies that include the full seasonal cycle of ozone in the Arctic are needed. In addition, a longer time series of ozone profiles over Summit Station would be helpful to determine if the conclusions of this study are robust.

Acknowledgments

We acknowledge useful discussions with Dr. Corinne Vigouroux from the Belgian Institute for Space Aeronomy that helped formulate the analysis for this study. We thank Detlev Helmig (University of Colorado - Institute of Arctic and Alpine Research) for helpful discussions regarding the operation and response time of ECC ozonesondes. We are grateful to Timothy Ginn (Washington State University) for his useful suggestions regarding stepwise multiple regression modelling. We acknowledge the Ozone and Water Vapor Group at the Earth System Research Laboratory of the National Oceanic and Atmospheric Administration for use of the ozonesonde data and the science technicians at Summit Station, Greenland for launching the ozonesondes. This research was supported by NSF grants PLR-1420932 and PLR-1414314.



References

- Allen, D. R., & Nakamura, N. (2003). Tracer Equivalent Latitude: A Diagnostic Tool for Isentropic Transport Studies. *J. Atmos. Sci.*, 60(2), 287–304. [http://doi.org/10.1175/1520-0469\(2003\)060<0287:teladt>2.0.co;2](http://doi.org/10.1175/1520-0469(2003)060<0287:teladt>2.0.co;2)
- 5 Ancellet, G., Daskalakis, N., Raut, J. C., Tarasick, D., Hair, J., Quennehen, B., Ravetta, F., Schlager, H., Weinheimer, A. J., Thompson, A. M., Johnson, B., Thomas, J. L. and Law, K. S.: Analysis of the latitudinal variability of tropospheric ozone in the Arctic using the large number of aircraft and ozonesonde observations in early summer 2008, *Atmos. Chem. Phys.*, 16(20), 13341–13358, doi:10.5194/acp-16-13341-2016, 2016.
- Anstey, J. A. and Shepherd, T. G.: High-latitude influence of the quasi-biennial oscillation, *Q. J. Royal Meteorol. Soc.*, 140, 1–21, doi:10.1002/qj.2132, 2014.
- 10 Appenzeller, C., Weiss, A. K. and Staehelin, J.: North Atlantic Oscillation modulates total ozone winter trends, *Geophys. Res. Lett.*, 27(8), 1131–1134, doi:10.1029/1999GL010854, 2000.
- Baldwin, M. P. and O'Sullivan, D.: Stratospheric Effects of ENSO-Related Tropospheric Circulation Anomalies, *J. Climate*, 8(4), 649–667, doi:10.1175/1520-0442(1995)008<0649:seoert>2.0.co;2, 1995.
- Ball, W. T., Alsing, J., Mortlock, D. J., Staehelin, J., Haigh, J. D., Peter, T., Tummon, F., Stübi, R., Stenke, A., Anderson, J., 15 Bourassa, A., Davis, S. M., Degenstein, D., Frith, S., Froidevaux, L., Roth, C., Sofieva, V., Wang, R., Wild, J., Yu, P., Ziemke, J. R., and Rozanov, E. V.: Evidence for a continuous decline in lower stratospheric ozone offsetting ozone layer recovery, *Atmos. Chem. Phys.*, 18, 1379–1394, <https://doi.org/10.5194/acp-18-1379-2018>, 2018.
- Bottenheim, J. W., Gallant, A. G. and Brice, K. A.: Measurements of NO_y species and O₃ at 82° N latitude, *Geophys. Res. Lett.*, 13(2), 113–116, doi:10.1029/GL013i002p00113, 1986.
- 20 Bottenheim, J. W., Fuentes, J. D., Tarasick, D. W. and Anlauf, K. G.: Ozone in the Arctic lower troposphere during winter and spring 2000 (ALERT2000), *Atmos. Environ.*, 36(1), 2535–2544, doi:10.1016/S1352-2310(02)00121-8, 2002.
- Bowman, K. P.: Global Patterns of the Quasi-biennial Oscillation in Total Ozone, *J. Atmos. Sci.*, 46(21), 3328–3343, doi:10.1175/1520-0469(1989)046<3328:gpotqb>2.0.co;2, 1989.
- Box, J. E. and Cohen, A. E.: Upper-air temperatures around Greenland: 1964–2005, *Geophys. Res. Lett.*, 33(12), 1829, 25 doi:10.1029/2006GL025723, 2006.
- Brunner, D., Staehelin, J., Maeder, J. A., Wohltmann, I. and Bodeker, G. E.: Variability and trends in total and vertically resolved stratospheric ozone based on the CATO ozone data set, *Atmos. Chem. Phys.*, 6(1), 4985–5008, doi:10.5194/acp-6-4985-2006, 2006.
- 30 Butchart, N., & Remsberg, E. E. (1986). The Area of the Stratospheric Polar Vortex as a Diagnostic for Tracer Transport on an Isentropic Surface. *J. Atmos. Sci.*, 43(13), 1319–1339. [http://doi.org/10.1175/1520-0469\(1986\)043<1319:taotsp>2.0.co;2](http://doi.org/10.1175/1520-0469(1986)043<1319:taotsp>2.0.co;2)



- Christiansen, B., Jepsen, N., Kivi, R., Hansen, G., Larsen, N., and Korsholm, U. S.: Trends and annual cycles in soundings of Arctic tropospheric ozone, *Atmos. Chem. Phys.*, 17, 9347-9364, <https://doi.org/10.5194/acp-17-9347-2017>, 2017.
- Cooper, O. R., Parrish, D. D., Stohl, A., Trainer, M., Nédélec, P., Thouret, V., Cammas, J. P., Oltmans, S. J., Johnson, B. J.,
5 Tarasick, D., Leblanc, T., McDermid, I. S., Jaffe, D., Gao, R., Stith, J., Ryerson, T., Aikin, K., Campos, T., Weinheimer, A. and Avery, M. A.: Increasing springtime ozone mixing ratios in the free troposphere over western North America, *Nature*, 463(7279), 344–348, doi:10.1038/nature08708, 2010.
- Crutzen, P. J.: Ozone production rates in an oxygen-hydrogen-nitrogen oxide atmosphere, *J. Geophys. Res.*, 76(30), 7311–7327, doi:10.1029/JC076i030p07311, 1971.
- 10 Damski, J., Thölix, L., Backman, L., Taalas, P., and Kulmala, M.: FinROSE - middle atmospheric chemistry and transport model, *Boreal Environ. Res.*, 12, 535-550, 2007.
- Danielsen, E. F. (1968). Stratospheric-Tropospheric Exchange Based on Radioactivity, Ozone and Potential Vorticity. *J. Atmos. Sci.*, 25(3), 502–518. [http://doi.org/10.1175/1520-0469\(1968\)025<0502:stebor>2.0.co;2](http://doi.org/10.1175/1520-0469(1968)025<0502:stebor>2.0.co;2)
- Deshler, T., Mercer, J., Smit, H., Stubi, R., Levrat, G., Johnson, B., Oltmans, S., Kivi, R., Thompson, A., Witte, J., Davies,
15 J., Schmidlin, F., Brothers, G., and Sasaki, T.: Atmospheric comparison of electrochemical cell ozonesondes from different manufacturers, and with different cathode solution strengths: The Balloon Experiment on Standards for Ozonesondes. *J. Geophys. Res.*, 113, D04307, doi:10.1029/2007JD008975, 2008.
- Deshler, T., Stübi, R., Schmidlin, F. J., Mercer, J. L., Smit, H. G. J., Johnson, B. J., Kivi, R., and Nardi, B.: Methods to homogenize electrochemical concentration cell (ECC) ozonesonde measurements across changes in sensing
20 solution concentration or ozonesonde manufacturer, *Atmos. Meas. Tech.*, 10, 2021-2043, <https://doi.org/10.5194/amt-10-2021-2017>, 2017.
- Forster, P. M. and Shine, K. P.: Radiative forcing and temperature trends from stratospheric ozone changes, *J. Geophys. Res.*, 102(D), 10841–10855, doi:10.1029/96JD03510, 1997.
- Doherty, R. M., Stevenson, D. S., Johnson, C. E., Collins, W. J. and Sanderson, M. G.: Tropospheric ozone and El Niño–
25 Southern Oscillation: Influence of atmospheric dynamics, biomass burning emissions, and future climate change, *J. Geophys. Res.*, 111(D19), 3867, doi:10.1029/2005JD006849, 2006.
- Ebdon, R. A.: The quasi-biennial oscillation and its association with tropospheric circulation pattern, *meteorological Magazine*, (104), 282–297, 1975.
- Eichelberger, S. J.: Changes in the strength of the Brewer-Dobson circulation in a simple AGCM, *Geophys. Res. Lett.*,
30 32(15), 1990–5, doi:10.1029/2005GL022924, 2005.
- Ettema, J., van den Broeke, M. R., van Meijgaard, E., van de Berg, W. J., Bamber, J. L., Box, J. E. and Bales, R. C.: Higher surface mass balance of the Greenland ice sheet revealed by high-resolution climate modeling, *Geophys. Res. Lett.*, 36(12), D06116, doi:10.1029/2009GL038110, 2009.



- Fusco, A. C. and Salby, M. L.: Interannual Variations of Total Ozone and Their Relationship to Variations of Planetary Wave Activity, *J. Climate*, 12(6), 1619–1629, doi:10.1175/1520-0442(1999)012<1619:ivotoa>2.0.co;2, 1999.
- Garfinkel, C. I. and Hartmann, D. L.: Effects of the El Niño–Southern Oscillation and the Quasi-Biennial Oscillation on polar temperatures in the stratosphere, *J. Geophys. Res.*, 112(D19), 3343–13, doi:10.1029/2007JD008481, 2007.
- 5 Garfinkel, C. I. and Hartmann, D. L.: Different ENSO teleconnections and their effects on the stratospheric polar vortex, *J. Geophys. Res.*, 113(D18), 30937–14, doi:10.1029/2008JD009920, 2008.
- Gaudel, A., Ancellet, G. and Godin-Beekmann, S.: Analysis of 20 years of tropospheric ozone vertical profiles by lidar and ECC at Observatoire de Haute Provence (OHP) at 44°N, 6.7 °E, *Atmos. Environ.*, 113(C), 78–89, doi:10.1016/j.atmosenv.2015.04.028, 2015.
- 10 Hanna, E., Navarro, F. J., Pattyn, F., Domingues, C. M., Fettweis, X., Ivins, E. R., Nicholls, R. J., Ritz, C., Ben Smith, Tulaczyk, S., Whitehouse, P. L. and Zwally, H. J.: Ice-sheet mass balance and climate change, *Nature*, 498(7452), 51–59, doi:10.1038/nature12238, 2013.
- Harris, N. R. P., Lehmann, R., Rex, M. and Gathen, von der, P.: A closer look at Arctic ozone loss and polar stratospheric clouds, *Atmospheric Chemistry and Physics*, 10(1), 8499–8510, doi:10.5194/acp-10-8499-2010, 2010.
- 15 Hasebe, F.: A Global Analysis of the Fluctuation of Total Ozone, *J. Meteor. Soc. Japan. Ser. II*, 58(2), 104–117, doi:10.2151/jmsj1965.58.2_104, 1980.
- Holton, J. R. and Lindzen, R. S.: An Updated Theory for the Quasi-Biennial Cycle of the Tropical Stratosphere, *J. Atmos. Sci.*, 29(6), 1076–1080, doi:10.1175/1520-0469(1972)029<1076:autftq>2.0.co;2, 1972.
- Holton, J. R. and Tan, H.-C.: The Influence of the Equatorial Quasi-Biennial Oscillation on the Global Circulation at 50 mb, *J. Atmos. Sci.*, 37(10), 2200–2208, doi:10.1175/1520-0469(1980)037<2200:tioteq>2.0.co;2, 1980.
- 20 Holton, J. R. and Tan, H.-C.: The Quasi-Biennial Oscillation in the Northern Hemisphere Lower Stratosphere, *J. Meteor. Soc. Japan. Ser. II*, 60(1), 140–148, doi:10.2151/jmsj1965.60.1_140, 1982.
- Holton, J. R., Haynes, P. H., McIntyre, M. E., Douglass, A. R., Rood, R. B. and Pfister, L.: Stratosphere-troposphere exchange, *Rev. Geophys.*, 33(4), 403–439, doi:10.1029/95RG02097, 1995.
- 25 Horowitz, L. W.: Past, present, and future concentrations of tropospheric ozone and aerosols: Methodology, ozone evaluation, and sensitivity to aerosol wet removal, *J. Geophys. Res.*, 111(D22), 955, doi:10.1029/2005JD006937, 2006.
- Jin, J. J., Semeniuk, K., Manney, G. L., Jonsson, A. I., Beagley, S. R., McConnell, J. C., Dufour, G., Nassar, R., Boone, C. D., Walker, K. A., Bernath, P. F. and Rinsland, C. P.: Severe Arctic ozone loss in the winter 2004/2005: observations from ACE-FTS, *Geophys. Res. Lett.*, 33(1), L15801, doi:10.1029/2006GL026752, 2006.
- 30 Johnson, B. J., Oltmans, S. J., Vömel, H., Smit, H. G. J., Deshler, T. and Kröger, C.: Electrochemical concentration cell (ECC) ozonesonde pump efficiency measurements and tests on the sensitivity to ozone of buffered and unbuffered ECC sensor cathode solutions, *J. Geophys. Res.*, 107(D19), 7881, doi:10.1029/2001JD000557, 2002.



- Kivi, R., Kyrö, E., Turunen, T., Harris, N. R. P., Gathen, von der, P., Rex, M., Andersen, S. B. and Wohltmann, I.: Ozonesonde observations in the Arctic during 1989–2003: Ozone variability and trends in the lower stratosphere and free troposphere, *J. Geophys. Res.*, 112(D8), 2013–17, doi:10.1029/2006JD007271, 2007.
- Komhyr, W. D.: Operations handbook-ozone measurements to 40-km altitude with Model 4A Electrochemical Concentration Cell (ECC) ozonesondes (used with 1680-MHz radiosondes), 1986.
- Komhyr, W. D., Grass, R. D. and Leonard, R. K.: Dobson spectrophotometer 83: A standard for total ozone measurements, 1962–1987, *J. Geophys. Res.*, 94(D7), 9847–9861, doi:10.1029/JD094iD07p09847, 1989.
- Li, K. F. and Tung, K. K.: Quasi-biennial oscillation and solar cycle influences on winter Arctic total ozone, *J. Geophys. Res.*, 119(10), 5823–5835, doi:10.1002/2013JD021065, 2014.
- Lindzen, R. S. and Holton, J. R.: A Theory of the Quasi-Biennial Oscillation, *J. Atmos. Sci.*, 25(6), 1095–1107, doi:10.1175/1520-0469(1968)025<1095:atotqb>2.0.co;2, 1968.
- Logan, J. A.: Trends in the vertical distribution of ozone: An analysis of ozonesonde data, *J. Geophys. Res.*, 99(D), 25–, doi:10.1029/94JD02333, 1994.
- Logan, J. A., Megretskaia, I. A., Miller, A. J., Tiao, G. C., Choi, D., Zhang, L., Stolarski, R. S., Labow, G. J., Hollandsworth, S. M., Bodeker, G. E., Claude, H., de Muer, D., Kerr, J. B., Tarasick, D. W., Oltmans, S. J., Johnson, B., Schmidlin, F., Staehelin, J., Viatte, P. and Uchino, O.: Trends in the vertical distribution of ozone: A comparison of two analyses of ozonesonde data, *J. Geophys. Res.*, 104(D), 26–, doi:10.1029/1999JD900300, 1999.
- Manney, G. L., Santee, M. L., Rex, M., Livesey, N. J., Pitts, M. C., Veefkind, P., Nash, E. R., Wohltmann, I., Lehmann, R., Froidevaux, L., Poole, L. R., Schoeberl, M. R., Haffner, D. P., Davies, J., Dorokhov, V., Gernandt, H., Johnson, B., Kivi, R., Kyrö, E., Larsen, N., Levelt, P. F., Makshtas, A., McElroy, C. T., Nakajima, H., Parrondo, M. C., Tarasick, D. W., Gathen, von der, P., Walker, K. A. and Zinoviev, N. S.: Unprecedented Arctic ozone loss in 2011, *Nature*, 478(7370), 469–475, doi:10.1038/nature10556, 2011. McClatchey, R. A.; Fenn, R. W.; Selby, J. E. A.; Volz, F. E.; Garing, J. S. Optical Properties of the Atmosphere, Air Force Cambridge Res. Lab.: L.G. Hanscom Field, Bedford, MA, AFCRL – 72 – 0497, 1972.
- McDonald, M. K., Turnbull, D. N. and Donovan, D. P.: Steller Brewer, ozonesonde, and DIAL measurements of Arctic O₃ column over Eureka, N.W.T. during 1996 winter/spring, *Geophys. Res. Lett.*, 26(15), 2383–2386, doi:10.1029/1999GL900506, 1999.
- McIntyre, M. E.: On the Antarctic ozone hole, *J. Atmospheric Sol.-Terr. Phys.*, 51(1), 29–43, doi:10.1016/0021-9169(89)90071-8, 1989.
- McPeters, R. D. and Labow, G. J.: Climatology 2011: An MLS and sonde derived ozone climatology for satellite retrieval algorithms, *J. Geophys. Res.*, 117(D10), doi:10.1029/2011JD017006, 2012.
- Miller, A. J., Cai, A., Tiao, G., Wuebbles, D. J., Flynn, L. E., Yang, S.-K., Weatherhead, E. C., Fioletov, V., Petropavlovskikh, I., Meng, X.-L., Guillas, S., Nagatani, R. M. and Reinsel, G. C.: Examination of ozonesonde data



- for trends and trend changes incorporating solar and Arctic oscillation signals, *J. Geophys. Res.*, 111(D), D13305, doi:10.1029/2005JD006684, 2006.
- Nair, P. J., Godin-Beekmann, S., Kuttippurath, J., Ancellet, G., Goutail, F., Pazmiño, A., Froidevaux, L., Zawodny, J. M., Evans, R. D., Wang, H. J., Anderson, J. and Pastel, M.: Ozone trends derived from the total column and vertical profiles at a northern mid-latitude station, *Atmos. Chem. Phys.*, 13(20), 10373–10384, doi:10.5194/acp-13-10373-2013, 2013.
- 5
- Newchurch, M. J.: Evidence for slowdown in stratospheric ozone loss: First stage of ozone recovery, *J. Geophys. Res.*, 108(D16), 23,079–13, doi:10.1029/2003JD003471, 2003.
- Randel, W. J., Garcia, R. R., Calvo, N. and Marsh, D.: ENSO influence on zonal mean temperature and ozone in the tropical lower stratosphere, *Geophys. Res. Lett.*, 36(15), n/a–n/a, doi:10.1029/2009GL039343, 2009.
- 10
- Rao, T. N.: Climatology of UTLS ozone and the ratio of ozone and potential vorticity over northern Europe, *J. Geophys. Res.*, 108(D22), 3451–10, doi:10.1029/2003JD003860, 2003.
- Rao, T. N., Arvelius, J., Kirkwood, S. and Gathen, von der, P.: Climatology of ozone in the troposphere and lower stratosphere over the European Arctic, *Adv. Space Res.*, 34(4), 754–758, doi:10.1016/j.asr.2003.05.055, 2004.
- 15
- Rex, M., Salawitch, R. J., Gathen, P. von der, Harris, N. R. P., Chipperfield, M. P., and Naujokat, B.: Arctic ozone loss and climate change, *Geophys. Res. Lett.*, 31(4), 4325–4, doi:10.1029/2003GL018844, 2004.
- Salby, M. L., and P. F. Callaghan, Fluctuations of total ozone and their relationship to stratospheric air motions, *J. Geophys. Res.*, 98(D2), 2715 – 2727, 1993.
- Shepherd, T. G.: Dynamics, stratospheric ozone, and climate change, *Atmosphere-Ocean*, 46(1), 117–138, doi:10.3137/ao.460106, 2008.
- 20
- Shindell, D. T., Chin, M., Dentener, F., Doherty, R. M., Faluvegi, G., Fiore, A. M., Hess, P., Koch, D. M., MacKenzie, I. A., Sanderson, M. G., Schultz, M. G., Schulz, M., Stevenson, D. S., Teich, H., Textor, C., Wild, O., Bergmann, D. J., Bey, I., Bian, H., Cuvelier, C., Duncan, B. N., Folberth, G., Horowitz, L. W., Jonson, J., Kaminski, J. W., Marmor, E., Park, R., Pringle, K. J., Schroeder, S., Szopa, S., Takemura, T., Zeng, G., Keating, T. J. and Zuber, A.: A multi-model assessment of pollution transport to the Arctic, *Atmos. Chem. Phys.*, 8(1), 5353–5372, doi:10.5194/acp-8-5353-2008, 2008.
- 25
- Smit, H. G. J., Straeter, W., Johnson, B. J., Oltmans, S. J., Davies, J., Tarasick, D. W., Hoegger, B., Stubi, R., Schmidlin, F. J., Northam, T., Thompson, A. M., Witte, J. C., Boyd, I. and Posny, F.: Assessment of the performance of ECC-ozonesondes under quasi-flight conditions in the environmental simulation chamber: Insights from the Juelich Ozone Sonde Intercomparison Experiment (JOSIE), *J. Geophys. Res.*, 112(D19), 563–18, doi:10.1029/2006JD007308, 2007.
- 30
- Solomon, S., Haskins, J., Ivy, D. J. and Min, F.: Fundamental differences between Arctic and Antarctic ozone depletion, *Proc. Natl. Acad. Sci. U.S.A.*, 111(17), 6220–6225, doi:10.1073/pnas.1319307111, 2014.



- Solomon, S., Portmann, R. W., Sasaki, T., Hofmann, D. J. and Thompson, D. W. J.: Four decades of ozonesonde measurements over Antarctica, *J. Geophys. Res.*, 110(D21), 25877–15, doi:10.1029/2005JD005917, 2005.
- Stachelin, J., Harris, N. R. P., Appenzeller, C. and Eberhard, J.: Ozone trends: A review, *Rev. Geophys.*, 39(2), 231–290, doi:10.1029/1999RG000059, 2001.
- 5 Steinbrecht, W., Claude, H., Köhler, U. and Hoinka, K. P.: Correlations between tropopause height and total ozone: Implications for long-term changes, *J. Geophys. Res.*, 103(D), 19–, doi:10.1029/98JD01929, 1998.
- Steinbrecht, W., Froidevaux, L., Fuller, R., Wang, R., Anderson, J., Roth, C., Bourassa, A., Degenstein, D., Damadeo, R., Zawodny, J., Frith, S., McPeters, R., Bhartia, P., Wild, J., Long, C., Davis, S., Rosenlof, K., Sofieva, V., Walker, K., Rahpoe, N., Rozanov, A., Weber, M., Laeng, A., Clarman, von, T., Stiller, G., Kramarova, N., Godin-Beekmann, S., Leblanc, T., Querel, R., Swart, D., Boyd, I., Hocke, K., Kämpfer, N., Maillard Barras, E., Moreira, L., Nedoluha, G., Vigouroux, C., Blumenstock, T., Schneider, M., Garcia, O., Jones, N., Mahieu, E., Smale, D., Kotkamp, M., Robinson, J., Petropavlovskikh, I., Harris, N., Hassler, B., Hubert, D. and Tummon, F.: An update on ozone profile trends for the period 2000 to 2016, *Atmos. Chem. Phys.*, 17(17), 10675–10690, doi:10.5194/acp-17-10675-2017, 2017.
- 10 Sterling, C. W., Johnson, B. J., Oltmans, S. J., Smit, H. G. J., Jordan, A. F., Cullis, P. D., Hall, E. G., Thompson, A. M. and Witte, J. C.: Homogenizing and Estimating the Uncertainty in NOAA’s Long Term Vertical Ozone Profile Records Measured with the Electrochemical Concentration Cell Ozonesonde, *Atmos. Meas. Tech. Discuss.*, 1–39, doi:10.5194/amt-2017-397, 2017.
- Sumner, A. L. and Shepson, P. B.: Snowpack production of formaldehyde and its effect on the Arctic troposphere, *Nature*, 20 398(6724), 230–233, doi:10.1038/18423, 1999.
- Taguchi, M. and Hartmann, D. L.: Increased Occurrence of Stratospheric Sudden Warmings during El Niño as Simulated by WACCM, *J. Climate*, 19(3), 324–332, doi:10.1175/jcli3655.1, 2006.
- Tarasick, D. W.: Changes in the vertical distribution of ozone over Canada from ozonesondes: 1980–2001, *J. Geophys. Res.*, 110(D2), 1131, doi:10.1029/2004JD004643, 2005.
- 25 Thompson, D. W. J., Baldwin, M. P. and Wallace, J. M.: Stratospheric Connection to Northern Hemisphere Wintertime Weather: Implications for Prediction, *J. Climate*, 15(1), 1421–1428, doi:10.1175/1520-0442(2002)015<1421:SCTNHW>2.0.CO;2, 2002.
- Van Dam, B., Helmig, D., Toro, C., Doskey, P., Kramer, L., Murray, K., Ganzeveld, L. and Seok, B.: Dynamics of ozone and nitrogen oxides at Summit, Greenland: I. Multi-year observations in the snowpack, *Atmos. Environ.*, 123, 268–30 284, doi:10.1016/j.atmosenv.2015.09.060, 2015.
- Van der A, R. J., Eskes, H. J., Boersma, K. F., van Noije, T. P. C., Van Roozendaal, M., De Smedt, I., Peters, D. H. M. U. and Meijer, E. W.: Trends, seasonal variability and dominant NO_x source derived from a ten year record of NO₂ measured from space, *J. Geophys. Res.*, 113(D4), 955, doi:10.1029/2007JD009021, 2008.



- Von Hobe, M., Bekki, S., Borrmann, S., Cairo, F., D'Amato, F., Di Donfrancesco, G., Dörnbrack, A., Ebersoldt, A., Ebert, M., Emde, C., Engel, I., Ern, M., Frey, W., Genco, S., Griessbach, S., Groß, J. U., Gulde, T., Günther, G., Hösen, E., Hoffmann, L., Homonnai, V., Hoyle, C. R., Isaksen, I. S. A., Jackson, D. R., Jánosi, I. M., Jones, R. L., Kandler, K., Kalicinsky, C., Keil, A., Khaykin, S. M., Khosrawi, F., Kivi, R., Kuttippurath, J., Laube, J. C., Lefevre, F.,
5 Lehmann, R., Ludmann, S., Luo, B. P., Marchand, M., Meyer, J., Mitev, V., Molleker, S., Müller, R., Oelhaf, H., Olschewski, F., Orsolini, Y., Peter, T., Pfeilsticker, K., Piesch, C., Pitts, M. C., Poole, L. R., Pope, F. D., Ravegnani, F., Rex, M., Riese, M., Röckmann, T., Rognerud, B., Roiger, A., Rolf, C., Santee, M. L., Scheibe, M., Schiller, C., Schlager, H., Siciliani de Cumis, M., Sitnikov, N., Søvde, O. A., Spang, R., Spelten, N., Stordal, F., Sumińska-Ebersoldt, O., Ulanovski, A., Ungermann, J., Viciani, S., Volk, C. M., Scheidt, vom, M., Gathen, von
10 der, P., Walker, K., Wegner, T., Weigel, R., Weinbruch, S., Wetzell, G., Wienhold, F. G., Wohltmann, I., Woiwode, W., Young, I. A. K., Yushkov, V., Zobrist, B. and Stroh, F.: Reconciliation of essential process parameters for an enhanced predictability of Arctic stratospheric ozone loss and its climate interactions (RECONCILE): activities and results, *Atmospheric Chemistry and Physics*, 13(1), 9233–9268, doi:10.5194/acp-13-9233-2013, 2013.
- Van Haver, P., De Muer, D., Beekmann, M. and Mancier, C.: Climatology of tropopause folds at midlatitudes, *Geophys. Res. Lett.*, 23(9), 1033–1036, doi:10.1029/96GL00956, 1996.
15
- Vigouroux, C., De Mazière, M., Demoulin, P., Servais, C., Hase, F., Blumenstock, T., Kramer, I., Schneider, M., Mellqvist, J., Strandberg, A., Velasco, V., Notholt, J., Sussmann, R., Stremme, W., Rockmann, A., Gardiner, T., Coleman, M. and Woods, P.: Evaluation of tropospheric and stratospheric ozone trends over Western Europe from ground-based FTIR network observations, *Atmos. Chem. Phys.*, 8(23), 6865–6886, doi:10.5194/acp-8-6865-2008, 2008.
- 20 Vigouroux, C., Blumenstock, T., Coffey, M., Errera, Q., García, O., Jones, N. B., Hannigan, J. W., Hase, F., Liley, B., Mahieu, E., Mellqvist, J., Notholt, J., Palm, M., Persson, G., Schneider, M., Servais, C., Smale, D., Thölix, L. and De Mazière, M.: Trends of ozone total columns and vertical distribution from FTIR observations at eight NDACC stations around the globe, *Atmos. Chem. Phys.*, 15(6), 2915–2933, doi:10.5194/acp-15-2915-2015, 2015.
- Wallace, J. M.: General circulation of the tropical lower stratosphere, *Rev. Geophys.*, 11(2), 191–222,
25 doi:10.1029/RG011i002p00191, 1973.
- Weber, M., Coldewey-Egbers, M., Fioletov, V. E., Frith, S. M., Wild, J. D., Burrows, J. P., Long, C.S., Loyola, D.: Total ozone trends from 1979 to 2016 derived from five merged observational datasets - the emergence into ozone recovery. *Atmos. Chem. Phys.*, 18(3), 2097–2117. <http://doi.org/10.5194/acp-18-2097-2018>, 2018.
- Weatherhead, E. C. and Andersen, S. B.: The search for signs of recovery of the ozone layer, *Nature*, 441(7), 39–45,
30 doi:10.1038/nature04746, 2006.
- Wilks, D. S., *Statistical Methods in the Atmospheric sciences*, 3rd edition. Elsevier, 676, 2011.
- WMO: Scientific assessment of ozone depletion: 2006. WMO Rep. 50, Global Ozone Research and Monitoring Project, 572, 2007. [Available online at http://www.wmo.int/pages/prog/arep/gaw/ozone_2006/ozone_asst_report.html.]



- WMO: Assessment for Decision-Makers Scientific Assessment of Ozone Depletion: 2014, WMO Rep. 55, 413, 2014.
[Available online at
http://www.wmo.int/pages/prog/arep/gaw/ozone_2014/documents/Full_report_2014_Ozone_Assessment.pdf]
- Wohlmann, I., Rex, M., Brunner, D., & Mäder, J. Integrated equivalent latitude as a proxy for dynamical changes in ozone
5 column. *Geophys. Res. Lett.*, 32(9), L09811. doi:10.1029/2005GL022497, 2005.
- Yang, E.-S., Cunnold, D. M., Salawitch, R. J., McCormick, M. P., Russell, J., III, Zawodny, J. M., Oltmans, S. and
Newchurch, M. J.: Attribution of recovery in lower-stratospheric ozone, *J. Geophys. Res.*, 111(D17), 8399,
doi:10.1029/2005JD006371, 2006.
- Yang, X., Pyle, J. A., Cox, R. A., Theys, N. and Van Roozendaal, M.: Snow-sourced bromine and its implications for polar
10 tropospheric ozone, *Atmos. Chem. Phys.*, 10(16), 7763–7773, doi:10.5194/acp-10-7763-2010, 2010.



Tables

Table 1: List of observing stations used for analysis in this study.

Station	Latitude	Longitude	Altitude (km)
Summit	73 N	38 E	3.22
Ny-Ålesund	79 N	12 E	0.02
Kiruna	68 N	20 E	0.42



5 **Table 2:** Effect of data screening on number of ozonesondes used each month in this study. “Total” contains the number of original ozonesondes from NOAA GMD, “Missing Data > 40%” contains the number of ozonesondes rejected because more than 40% of data in the vertical profile is missing, “Burst altitude < 18 km” contains the number of ozonesonde rejected because the burst altitude of the sonde balloon was below 18 km. “Retained for analysis” shows the number of ozonesondes that were retained for data analysis.

Month	Total	More than >40%	Burst altitude < 18 km	Retained for analysis
January	46	1	21	25 (54%)
February	54	2	11	43 (80%)
March	70	2	5	65 (93%)
April	42	0	0	42 (100%)
May	48	0	0	48 (100%)
Jun	42	1	3	39 (93%)
July	39	1	4	34 (87%)
August	43	0	0	43 (100%)
September	42	2	3	39 (93%)
October	46	3	7	39 (85%)
November	46	1	5	41 (89%)
December	45	2	13	32 (71%)


Table 3: Proxies used in the stepwise multiple regression performed in this study to explain variance in the total column ozone amount over Summit Station, Greenland.

	Description	Source
Tropopause pressure (TP)	Derived from NCEP/NCAR reanalysis data from NOAA's Earth System Research Laboratory	https://www.esrl.noaa.gov/psd/cgi-bin/db_search/DBSearch.pl?Dataset=CDC+Derived+NCEP+Reanalysis+Products+Tropopause+Level&Variable=Pressure&group=0&submit=Search
Quasi-biennial oscillation (QBO)	Based on equatorial stratosphere winds at 30 and 10 hpa	http://www.geo.fu-berlin.de/en/met/ag/strat/produkte/qbo/index.html
Volume polar stratospheric cloud (VPSC)	Calculated between 375 and 550K potential temperature	Calculated at FMI using chemistry and transport model FinROSE (Damski et al., 2007)
Eddy heat flux (EHF)	Averaged over 45-75 N at 100 hP	https://acd-ext.gsfc.nasa.gov/Data_services/met/ann_data.html
Arctic oscillation (AO)		http://www.cpc.ncep.noaa.gov/products/precip/CWlink/daily_ao_index/ao.shtml
Equivalent latitude (EQL)	At 3 altitude levels of potential temperature 370K, 550K, 960K	Calculated at FMI
EESC	Mean age of air 5.3 years	https://acd-ext.gsfc.nasa.gov/Data_services/automailer/restricted/eesc.php
Solar flux		ftp://ftp.ngdc.noaa.gov/STP/space-weather/solar-data/solar-features/solar-radio/noontime-flux/penticton/penticton_observed/tables/table_drao_noontime-flux-observed_monthly.txt
Multivariate ENSO index (MEI)		http://www.esrl.noaa.gov/psd/enso/mei/



Table 4: Correlation of determination for the seasonal cycle and final regression model of ozone variations over Summit Station, Greenland (2005-2016).

	Sfc-10 km	10-18 km	18-27 km	27-42 km	Total Column
Seasonal cycle model R^2 (%)	55	68	53	73	68
Final regression model, R^2 (in %)	77	84	69	77	84



5 **Table 5:** The correlation of determination (R^2) in % obtained in the stepwise multiple regression analysis. The regression is performed on the residual ozone time series after subtracting the seasonal cycle. The R^2 values are listed in order of importance in the descending order. Proxies with could not improve the R^2 more than 1% are excluded from model and shown here as <1. Proxies such as Solar flux, EQL and ENSO that found insignificant in all layers are not listed. The sign next to the R^2 value is the sign of the slope of the regression. The R^2 of the final residual model for each atmospheric layer is shown in the bottom row. The sign of the QBO is not shown because its contribution comes from several different terms and a single slope sign is, thus, not applicable for this proxy.

Sfc-10 (km)		10-18 (km)		18-27 (km)		27-42 (km)		Total Column	
<i>Proxy</i>	R^2	<i>Proxy</i>	R^2	<i>Proxy</i>	R^2	<i>Proxy</i>	R^2	<i>Proxy</i>	R^2
TP	35.4, +	TP	27.5, +	TP	10.6, +	EHF	5.1, +	TP	30.0, +
EHF	2.7, -	QBO	7.0	QBO	8.8	VPSC	4.3, -	VPSC	6.3, -
QBO	1.3	AO	4.6, +	VPSC	6.6, -	TP	2.7, +	QBO	6.0
AO	<1	VPSC	2.5, -	EHF	4.7, +	QBO	2.5	Trend	1.6, +
Trend	<1	Trend	1.3, +	Trend	1.2, +	Trend	<1	EHF	1.9, +
VPSC	<1	EHF	<1	AO	1.1, -	AO	<1	AO	<1
Total R^2	39.4		45.9		33.1		14.5		45.6



Figures

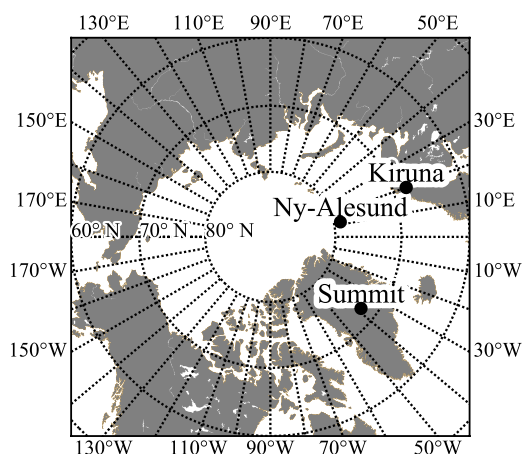
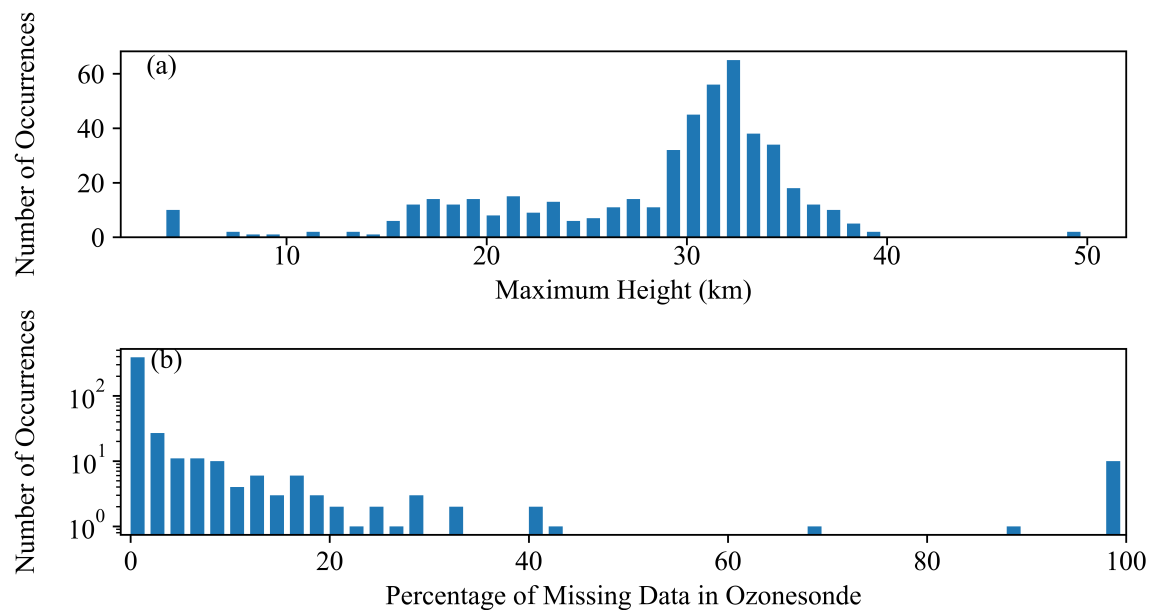


Figure 1: Map showing the locations of study sites used: Summit Station Greenland, Ny-Ålesund Svalbard, and Kiruna Sweden.



5 Figure 2: Characteristics of ozonesondes launched at Summit Station, Greenland between 2005 and 2016. a) Histogram of the maximum height reached by each ozonesonde. b) Histogram of the percentage of missing data in each ozonesonde.

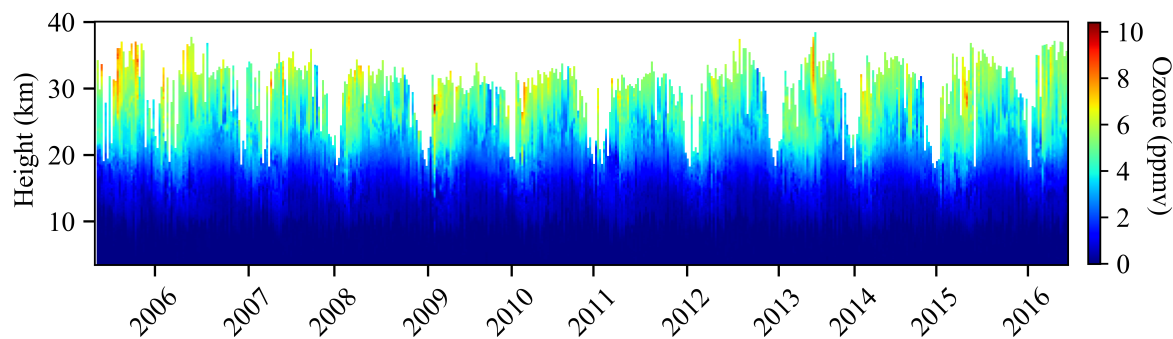
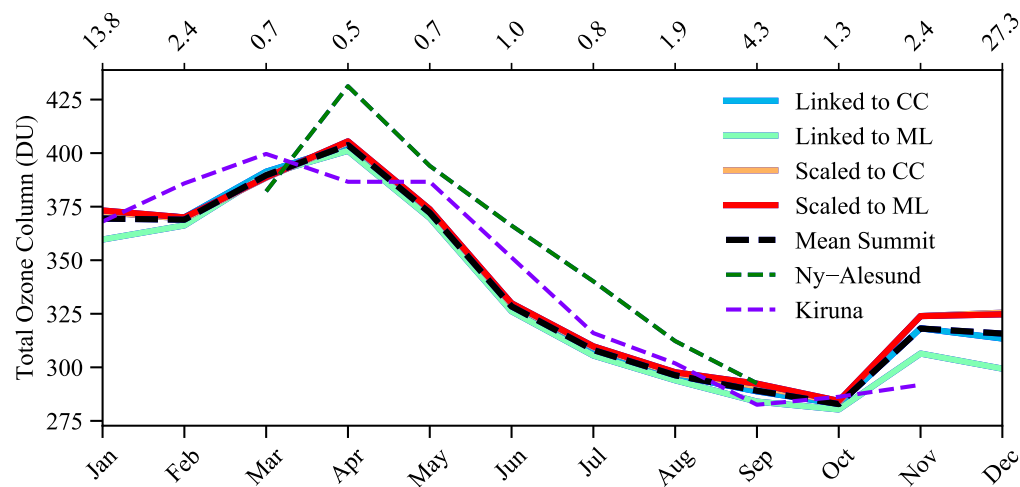


Figure 3: Profiles of ozone (in ppmv) measured by NOAA ozonesondes that have been screened and retained for data analysis. The maximum heights achieved in winter are lower than other times of year due to premature balloon bursts.



5 **Figure 4: Monthly mean total column ozone using four different methods for extrapolating climatological ozone above the measured ozonesonde profiles. The four methods are explained in the text, but involve either linking or scaling the calculated climatology (CC) based on the average ozonesonde profile or ML climatology (McPeters and Labow, 2012). The mean of the four methods is shown as the black dashed line. The values shown along the top axis are the monthly averages of the standard deviations of the total column ozone of the four constructed profiles (as explained in the text). The monthly mean total column ozone for Kiruna, Sweden and Ny-Ålesund, Svalbard are also shown based on Vigouroux et al (2008).**

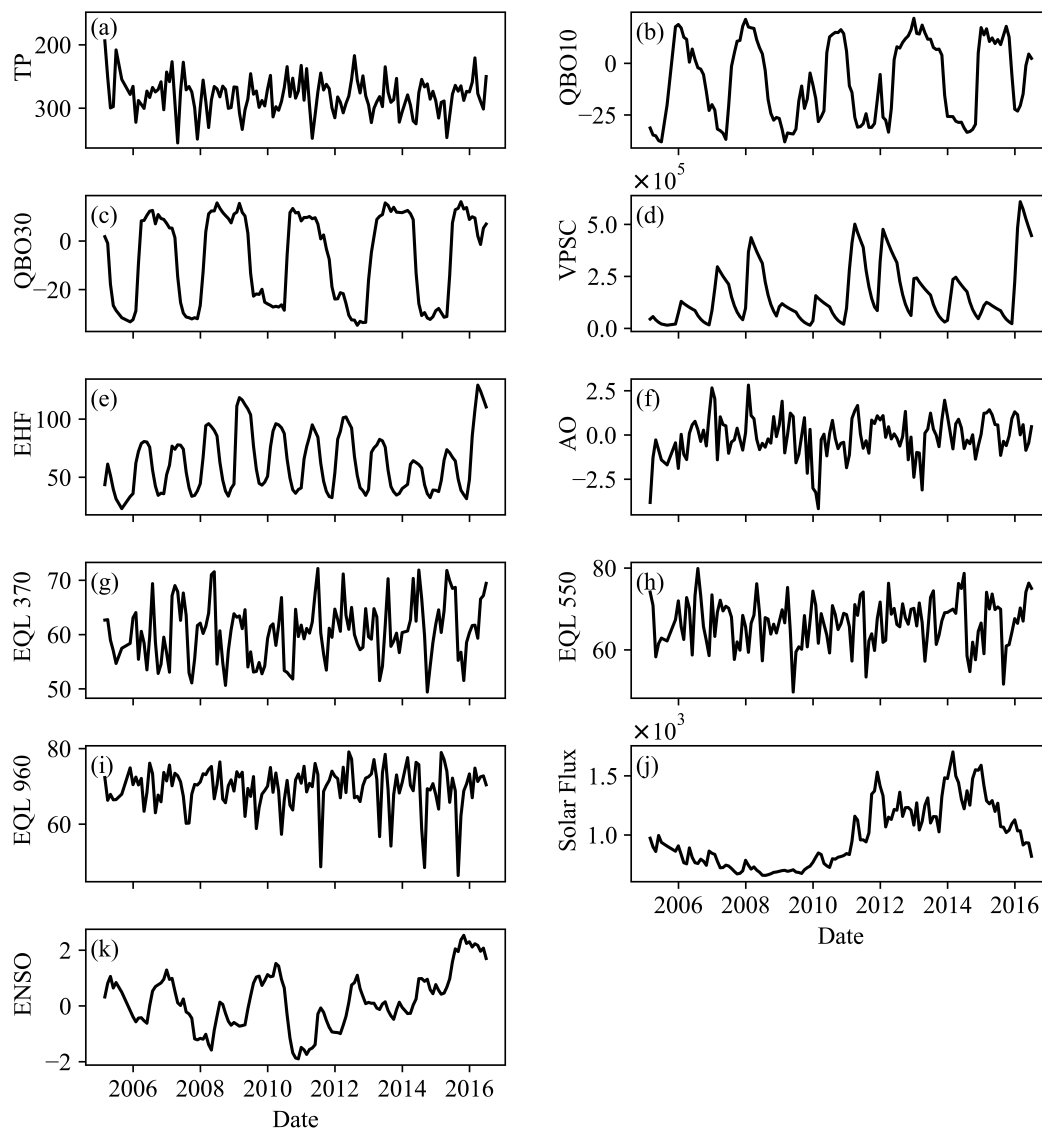
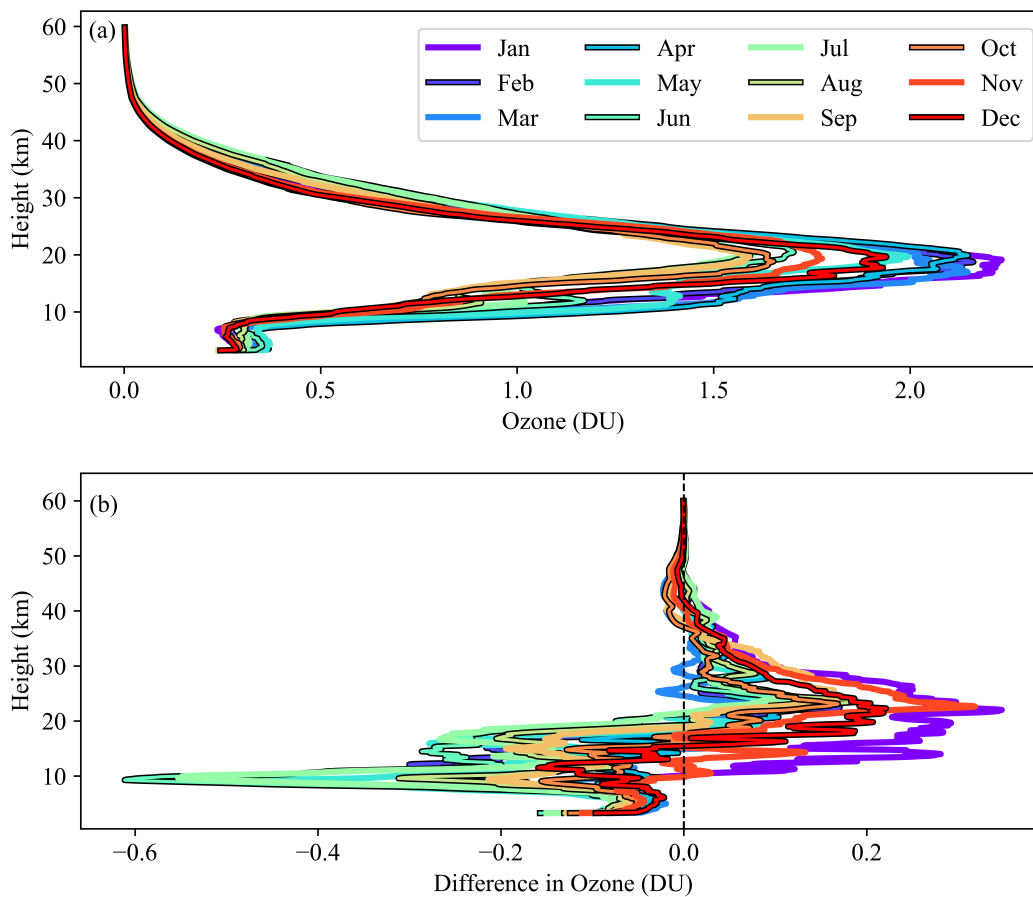


Figure 5: Time series of the proxies used in this study to analyze ozone variations over Summit Station, Greenland. The sources of the proxies are listed in Table 3. The units of the proxies: are unitless for ENSO and AO; m/s for QBO10 and QBO30 (positive values are westerly zonal winds, negative values are easterlies); W m^{-2} for Solar Flux and Eddy Heat Flux (EHF), hPa for Tropopause Pressure (TP), 10^6 km^3 for Volume of Polar Stratospheric Clouds (VPSC), and degrees for equivalent latitude (EQL) at potential temperatures of 370, 550, and 960 K. The proxy for VPSC is actually the cumulative volume of polar stratospheric clouds times the effective equivalent stratospheric chlorine (EESC) and cumulative EHF is named EHF (Brunner et al., 2006), as explained in the text.

5



5 **Figure 6:** a) Monthly average profiles of partial column ozone for each 100-meter layer over Summit Station, Greenland (2005-2016). b) Difference between the monthly average partial column ozone profiles at Summit and the ML climatology from McPeters and Labow (2012).

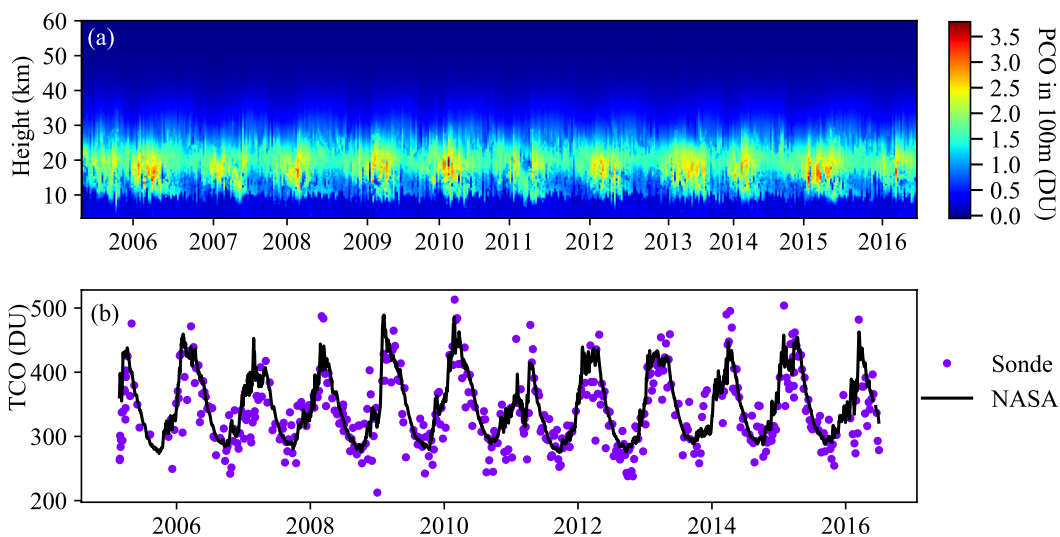


Figure 7: Time series of ozone variations over Summit Station, Greenland from 2005 to 2016. a) Partial column ozone (PCO) for each 100-meter layer. b) Purple points are the total column ozone (TCO) calculated from the vertical profiles. The black line is the average TCO for the Arctic (latitudes > 63 N) obtained from NASA's Arctic Ozone Watch. Note that the time scales are different for the two panels. The time scale for panel (a) is approximate to avoid gaps between the plotted profiles, while the time scale for panel (b) is accurate.

5

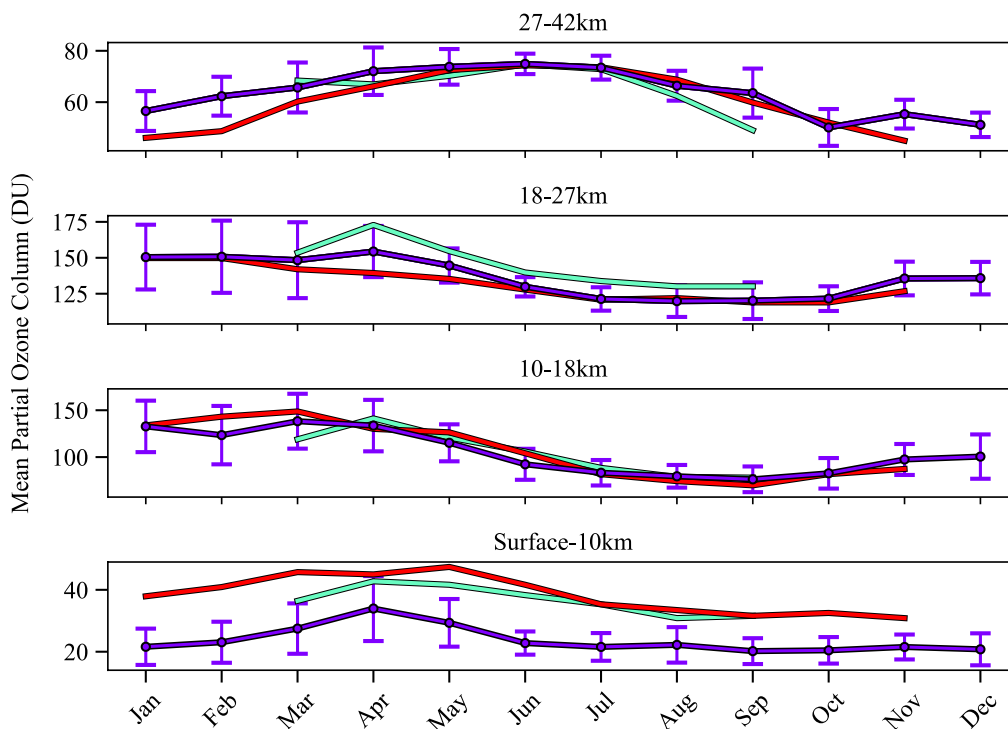


Figure 8: Partial ozone columns (PCOs) for different altitude layers at Summit Station, Greenland (purple). PCO values are also shown for Ny-Ålesund, Svalbard (green), and Kiruna, Sweden (red). The altitude is relative to sea level. The uncertainty bars for Summit Station represent the standard deviation of the monthly average from 2005 to 2016. The corresponding values for Ny-Ålesund and Kiruna are from Vigouroux et al. (2008) and are shown for comparison.

5

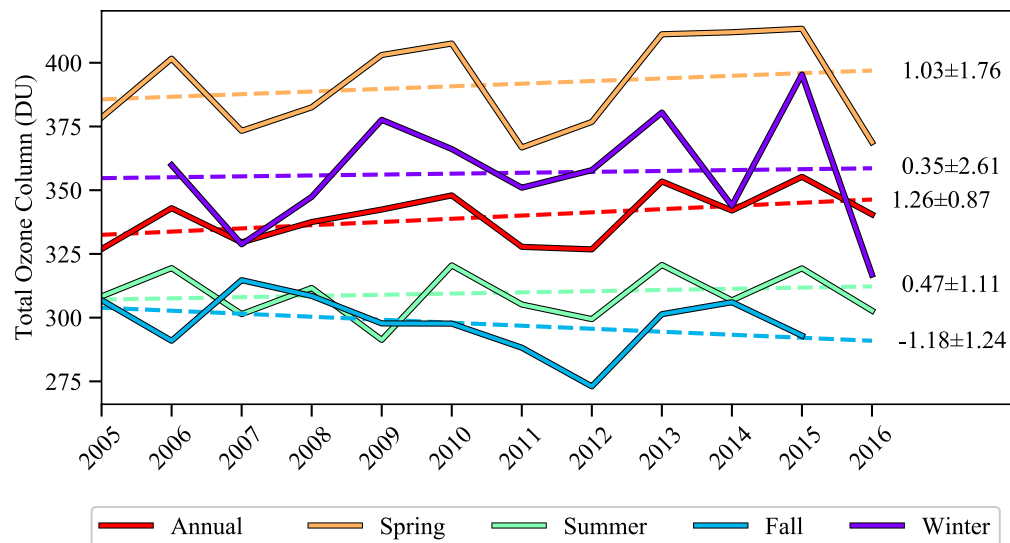


Figure 9: Trends in the annual and seasonal average total column ozone over Summit Station, Greenland. The annual trend is shown in red; the seasonal trends are shown in yellow (spring), green (summer), fall (cya), and winter (purple). The numbers at the right of each curve show the linear trend (slope) and the uncertainty in those trends obtained from linear regression. (Caution should be used when considering the significance of these trends due to the relatively short time period over which they were computed.)

5

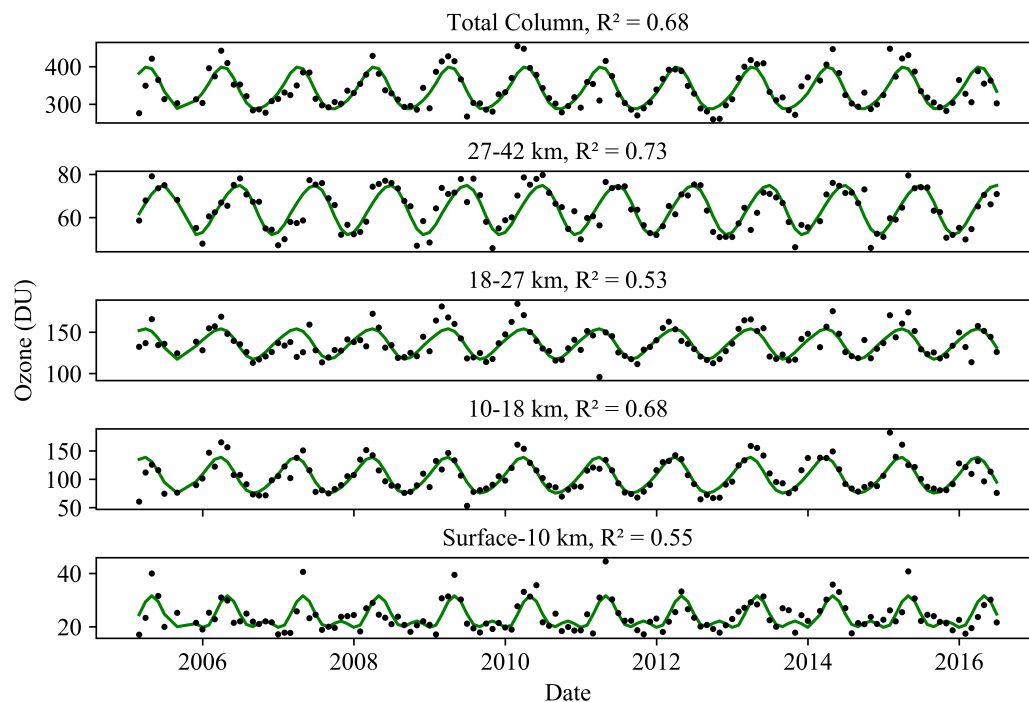


Figure 10: Time series of the total column ozone (top panel) and the partial column ozone in four atmospheric layers (four bottom panels) from Summit Station, Greenland (black dots). The fitted seasonal cycle is shown as the green curve. The coefficient of determination (R^2) for each seasonal fit is shown in the title for each panel.

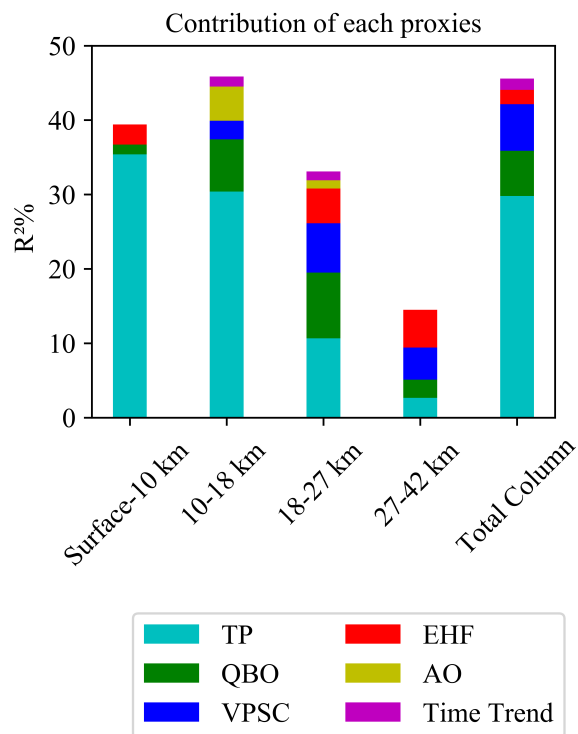


Figure 11: The contributions of the individual proxies determined by stepwise multiple regression (SMR) analysis for the four atmosphere layers (surface to 10 km, 10-18 km, 18-27 km, 27-42 km) and the total column ozone. [TP – Tropopause Pressure, QBO – Quasi-biennial oscillation, VPSC – Volume of Polar Stratospheric Clouds, EHF – Eddy Heat Flux, and AO – Arctic Oscillation]

5

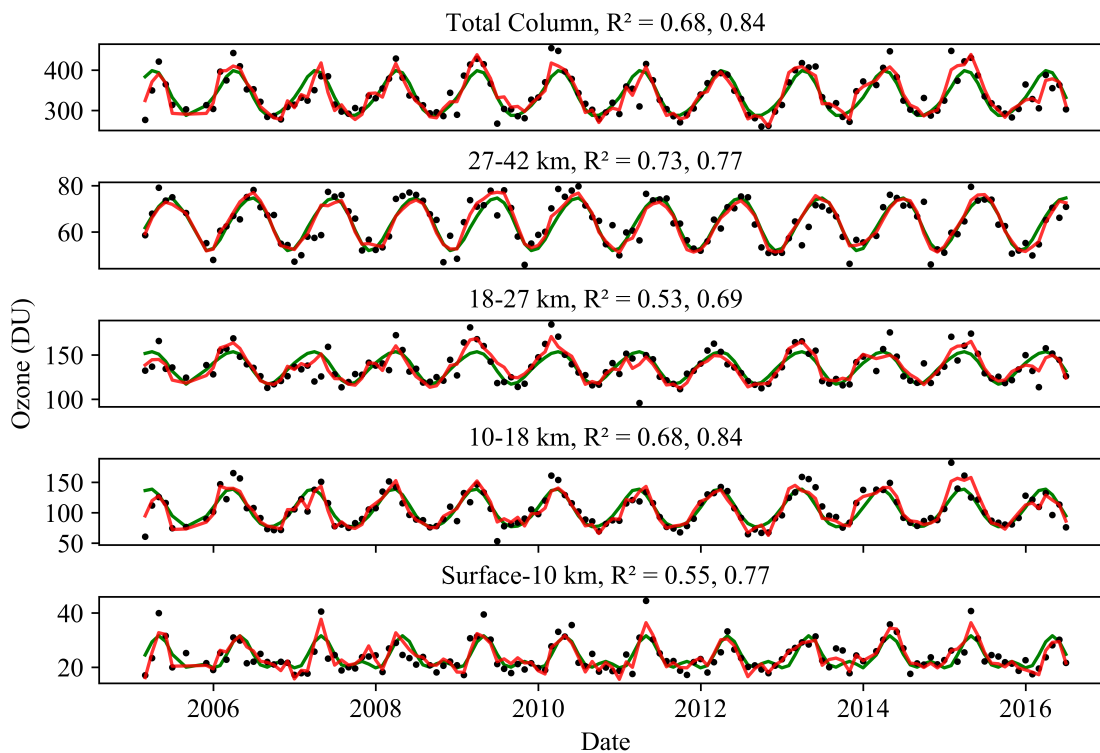


Figure 12: The results of the final regression model (red curve) of ozone variations over Summit Station, Greenland. The black dots are the original time series of the total column ozone and the partial column ozone from Figure 10. The fitted seasonal cycle is shown for reference as the green curve. The coefficient of determination (R^2) for each seasonal fit and for the final regression model are shown in the title for each panel.

5